

On the possibility of active control of instability waves in unexcited turbulent jets

Victor Kopiev, Georgy Faranosov, Sergey Chernyshev, Oleg Bychkov

Central Aerohydrodynamic Institute (TsAGI),
Moscow, Russia,

Outline

- Introduction
- Artificial instability waves (AIW) , AIW control strategy
- NIW control idea, Overview of LES-results,
- Data analysis in the jet shear layer
- Data analysis in the jet near field
- Experimental data
- NIW Control strategy
- Conclusion

Outline

- Introduction
- Artificial instability waves (AIW) , AIW control strategy
- NIW control idea, Overview of LES-results,
- Data analysis in the jet shear layer
- Data analysis in the jet near field
- Experimental data
- NIW Control strategy
- Conclusion

ISSN 0015-4628, Fluid Dynamics, 2018, Vol. 53, No. 3, pp. 347-360. © Pleiades Publishing, Ltd., 2018.
Original Russian Text © I.V. Belyaev, O.P. Bychkov, M.Yu. Zaitsev, V.A. Kopiev, V.F. Kopiev, N.N. Ostrikov, G.A. Faranosov, S.A. Chernyshev, 2018, published in
Izvestiya Rossiiskoi Akademii Nauk, Mekhanika Zhidkosti i Gaza, 2018, No. 3, pp. 14-27.

Development of the Strategy of Active Control of Instability Waves in Unexcited Turbulent Jets

I. V. Belyaev, O. P. Bychkov, M. Yu. Zaitsev, V. A. Kopiev,
V. F. Kopiev, N. N. Ostrikov, G. A. Faranosov*, and S. A. Chernyshev

*Central Aerodynamic Institute (TsAGI), Moscow Complex,
ul. Radio 17, Moscow, 107005, Russia*

Received November 10, 2017

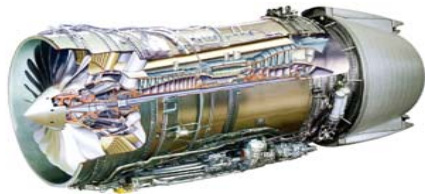
Examples of active/passive control of jet noise

Jet noise

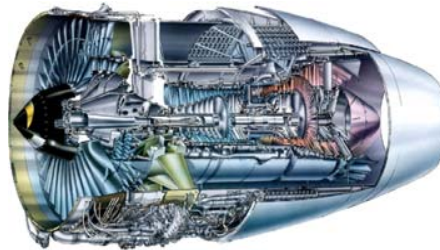
Lighthill's theory – acoustic power $\sim U^8$

Jet noise reduction – **increasing of BPR**

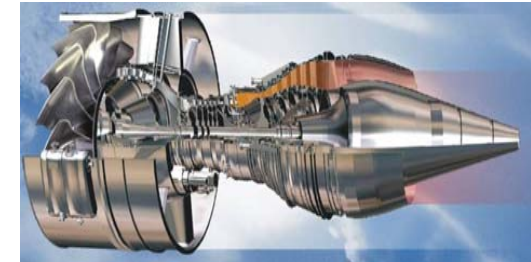
D-30KP



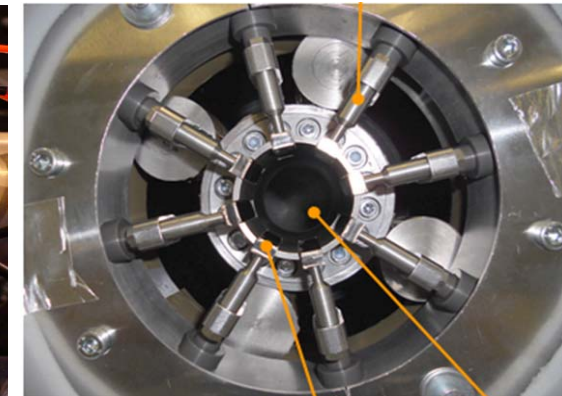
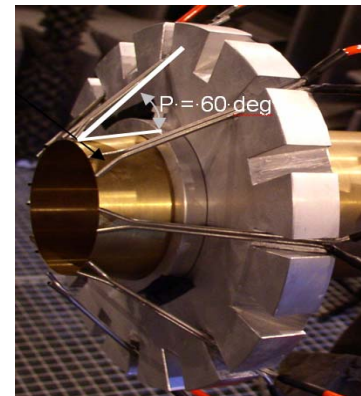
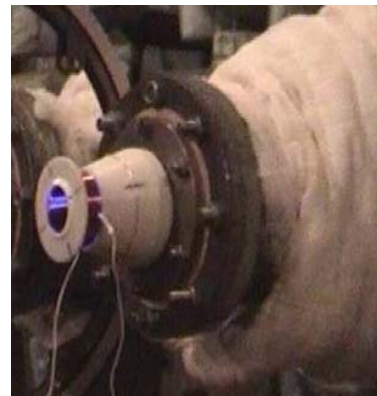
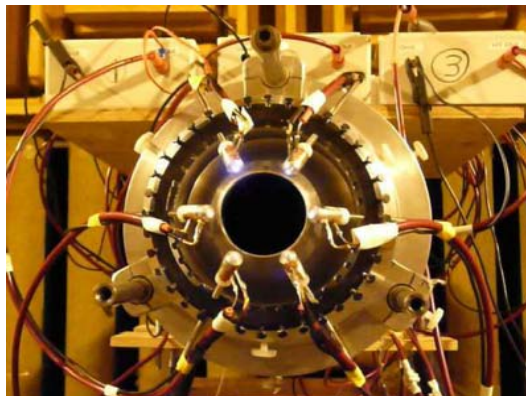
PS-90A



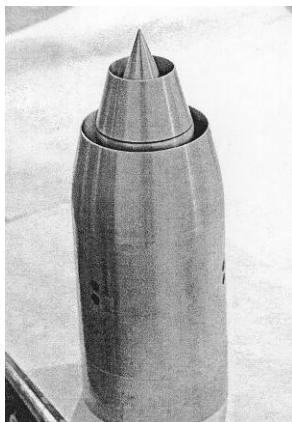
PD-14



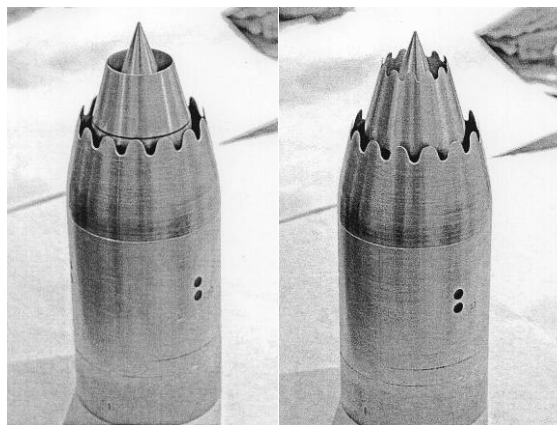
Active jet noise control



Nozzles with chevrons



Nozzles without chevrons



Chevrons directed streamwise



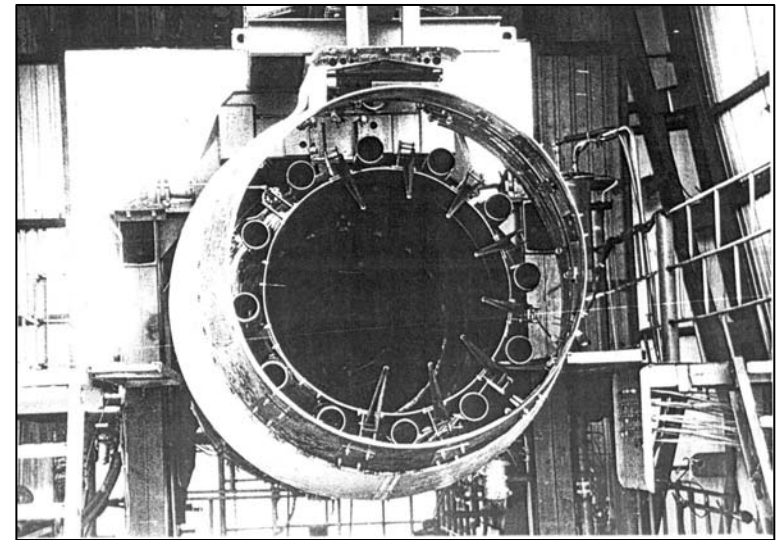
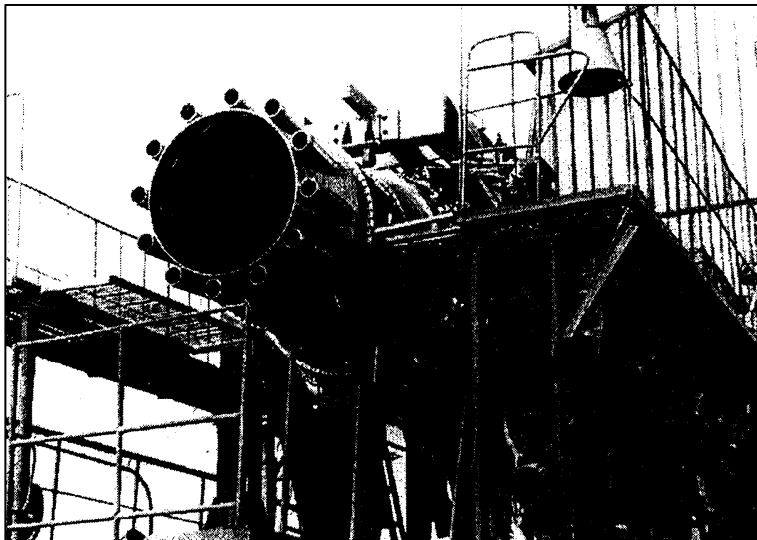
Chevrons deflected into the flow



Full-scale jet noise control - High TRL

Concept: It is known that low frequency noise excitation leads to broadband intensification of jet noise, vice versa high frequency excitation leads to noise suppression (at least for not very high amplitude of excitation) – low TRL experiments in anechoic chamber. Therefore high frequency excitation could be considered as a way for jet noise reduction

High TRL realization of this active control concept is presented on the picture for Nikolay Kuznetsov's type engine (NK): small-size jets located around main jet radiate more high-frequency noise compared the main jet, which acting on the main jet give mentioned suppression effect up to 3dB.



Instability wave control

AIW and NIW

Artificial instability waves (AIW)

AIW are tone excited NIW (natural instability waves).

AIW as multiple increased NIW are dominates in the narrow frequency band.

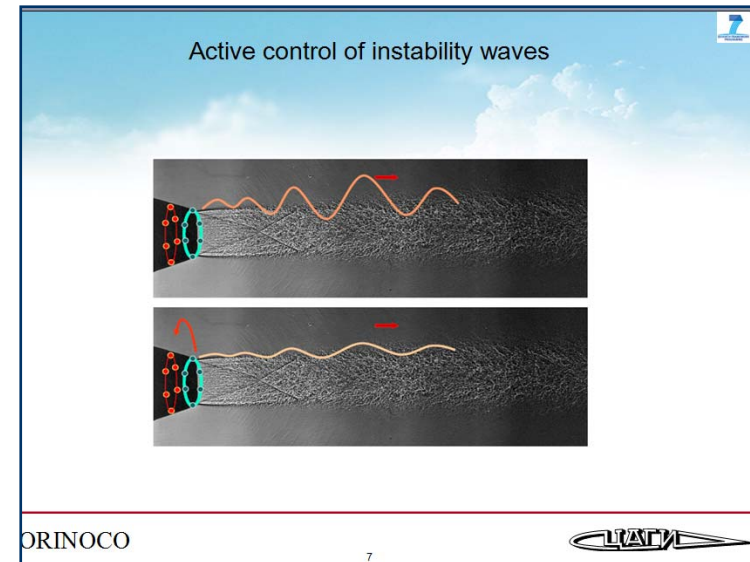
AIW have the same properties as NIW

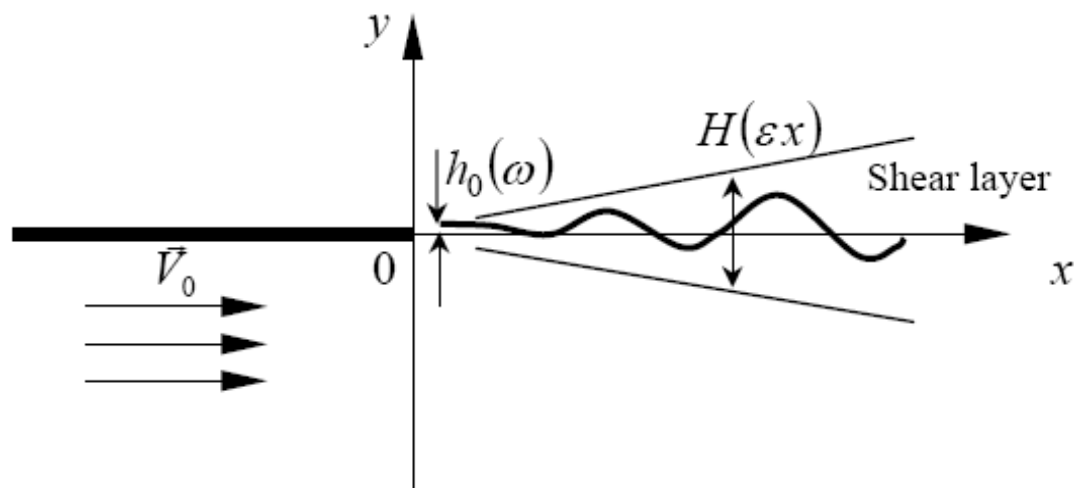
Benefits:

Easy to measure (hotwire, PIV)

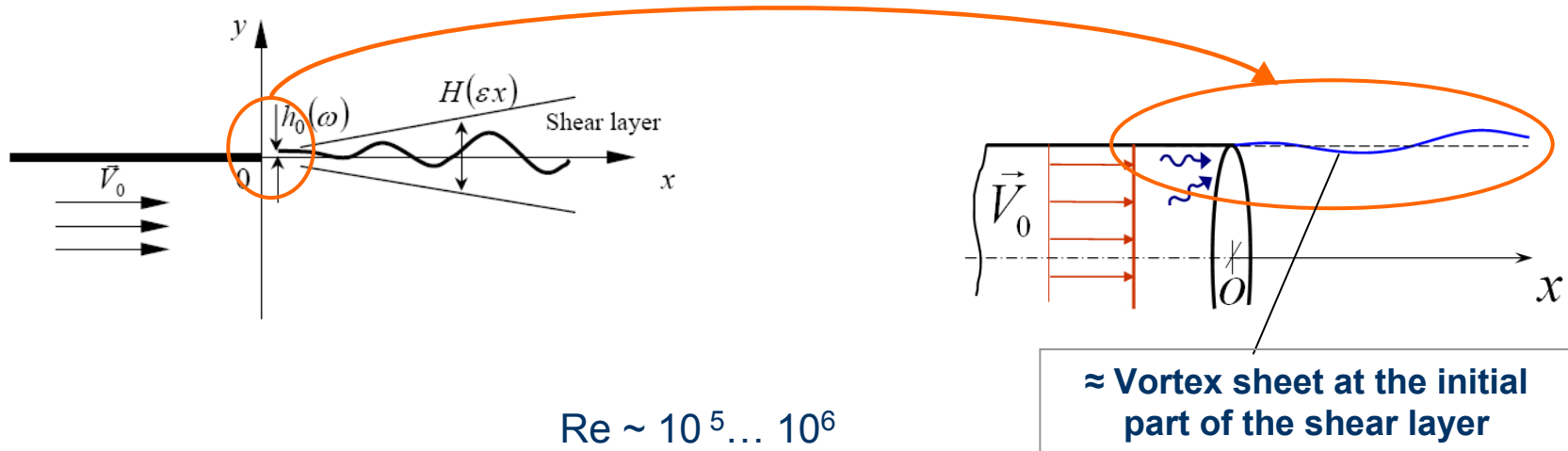
Easy to generate

Easy to control





Kelvin-Helmholtz instability waves (IW) in jet shear layer



Sedel'nikov T.K. The frequency spectrum of the noise of a supersonic jet // Phys. Aero. Noise Moscow: Nauka. 1967 (Trans. 1969 NASA TTF-538, P.71-75.)

Tam C.K.W., Burton D.E. Sound generated by instability waves of supersonic flows // J. Fluid Mech. 1984. V.138. P.249-295.

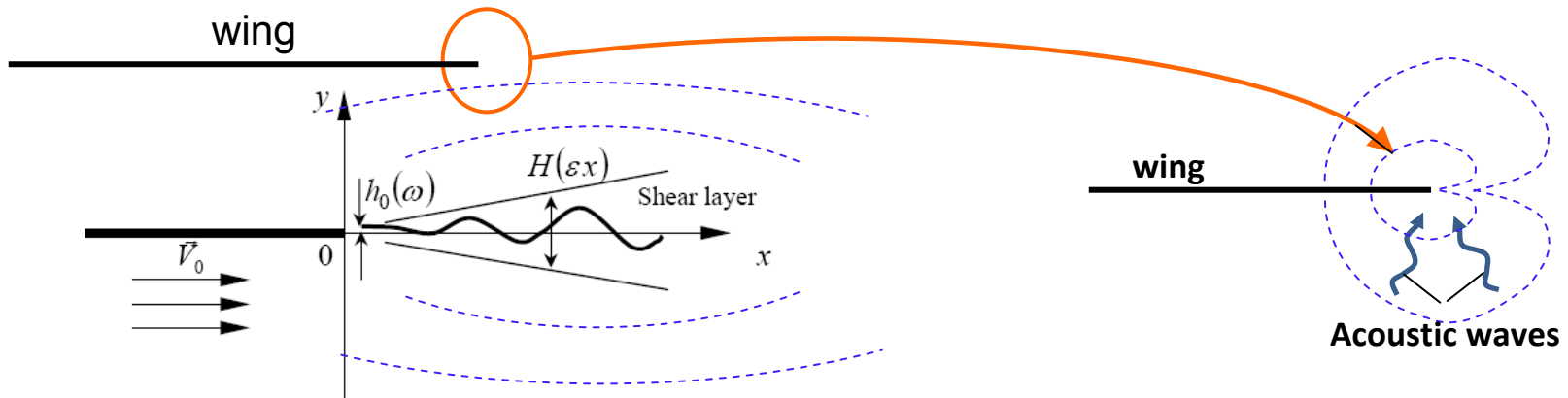
Crighton D.G., Huerre P. Shear-layer pressure fluctuations and superdirective acoustic sources // J. Fluid Mech. 1990. V.220. P.355-368.

Suzuki T., Colonius T. Instability waves in a subsonic round jet detected using a near-field phased microphone array // J. Fluid Mech. 2006. V.565. P.197-226.

Zaitsev M.Yu., Kopiev V.F., Chernyshev S.A. Experimental investigation of the role of instability waves in noise radiation by supersonic jets // Fluid Dynamics. 2009. V.44, N.4, P.587-595.

Morris P.J. The instability of high speed jets // Int. J. Aeroacoustics. 2010. V.9. N.1-2. P.1-50

Kelvin-Helmholtz instability waves (IW) in jet shear layer



$$\text{Re} \sim 10^5 \dots 10^6$$

Sedel'nikov T.K. The frequency spectrum of the noise of a supersonic jet // Phys. Aero. Noise Moscow: Nauka. 1967 (Trans. 1969 NASA TTF-538, P.71-75.)

Tam C.K.W., Burton D.E. Sound generated by instability waves of supersonic flows // J. Fluid Mech. 1984. V.138. P.249-295.

Crighton D.G., Huerre P. Shear-layer pressure fluctuations and superdirective acoustic sources // J. Fluid Mech. 1990. V.220. P.355-368.

Suzuki T., Colonius T. Instability waves in a subsonic round jet detected using a near-field phased microphone array // J. Fluid Mech. 2006. V.565. P.197-226.

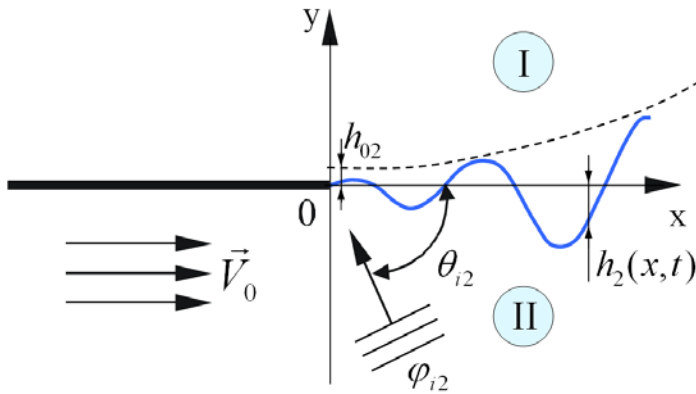
Zaitsev M.Yu., Kopiev V.F., Chernyshev S.A. Experimental investigation of the role of instability waves in noise radiation by supersonic jets // Fluid Dynamics. 2009. V.44, N.4, P.587-595.

Morris P.J. The instability of high speed jets // Int. J. Aeroacoustics. 2010. V.9. N.1-2. P.1-50

Outline

- Introduction
- **Artificial instability waves (AIW) , AIW control strategy**
- NIW control idea, Overview of LES-results,
- Data analysis in the jet shear layer
- Data analysis in the jet near field
- Experimental data
- NIW Control strategy
- Conclusion

Governing Eqs for 2D problem



$$\begin{cases} \Delta \varphi_I + k^2 \varphi_I = 0, & y > 0 \\ \Delta \varphi_{II} - \left(-ik + M \frac{\partial}{\partial x} \right)^2 \varphi_{II} = 0, & y < 0 \end{cases}$$

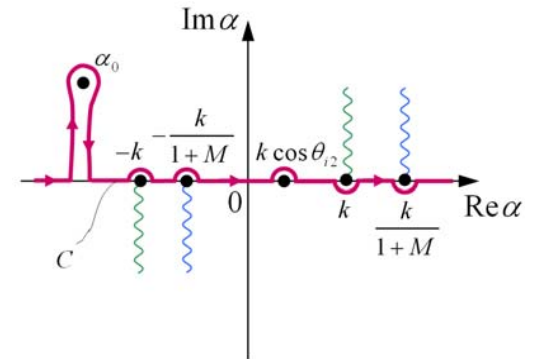
$$\varphi \sim \exp(i\alpha x - ikct)$$

$$\begin{aligned} \varphi &\sim \exp(-\gamma y) \\ \varphi &\sim \exp(\beta y) \end{aligned}$$

$$\begin{aligned} \gamma &= \sqrt{\alpha^2 - k^2} \\ \beta &= \sqrt{(\alpha(1+M) + k)(\alpha(1-M) - k)} \end{aligned}$$

$$\Phi(\alpha, y, k) = \int_{-\infty}^{+\infty} \varphi(x, y, k) \exp(i\alpha x) dx$$

$$\varphi(x, y, t) = A \cdot e^{-ikct} \int_C \Phi(\alpha, y, k) e^{-i\alpha x} d\alpha$$



$\Delta(k, \alpha) \equiv k^2 \beta + (k + M \alpha)^2 \gamma = 0$ ← Roots of this Eq. are the singularities of Φ

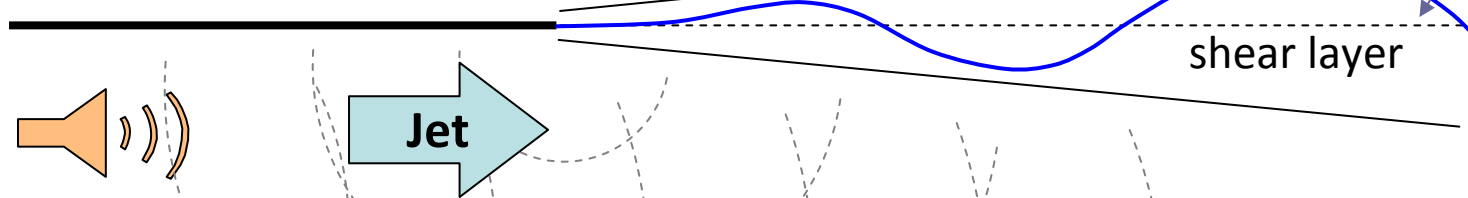
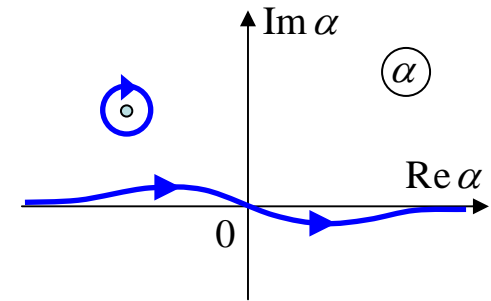
$$p_{inner}(\vec{r}, t) = B \cdot e^{-i\omega t} \int_{-\infty}^{+\infty} f_{inner}(\alpha, y) e^{-i\alpha x} d\alpha$$

Acoustic part

$$p_{inner}(\vec{r}, t) = B \cdot e^{-i\omega t} \int_C f_{inner}(\alpha, y) e^{-i\alpha x} d\alpha$$

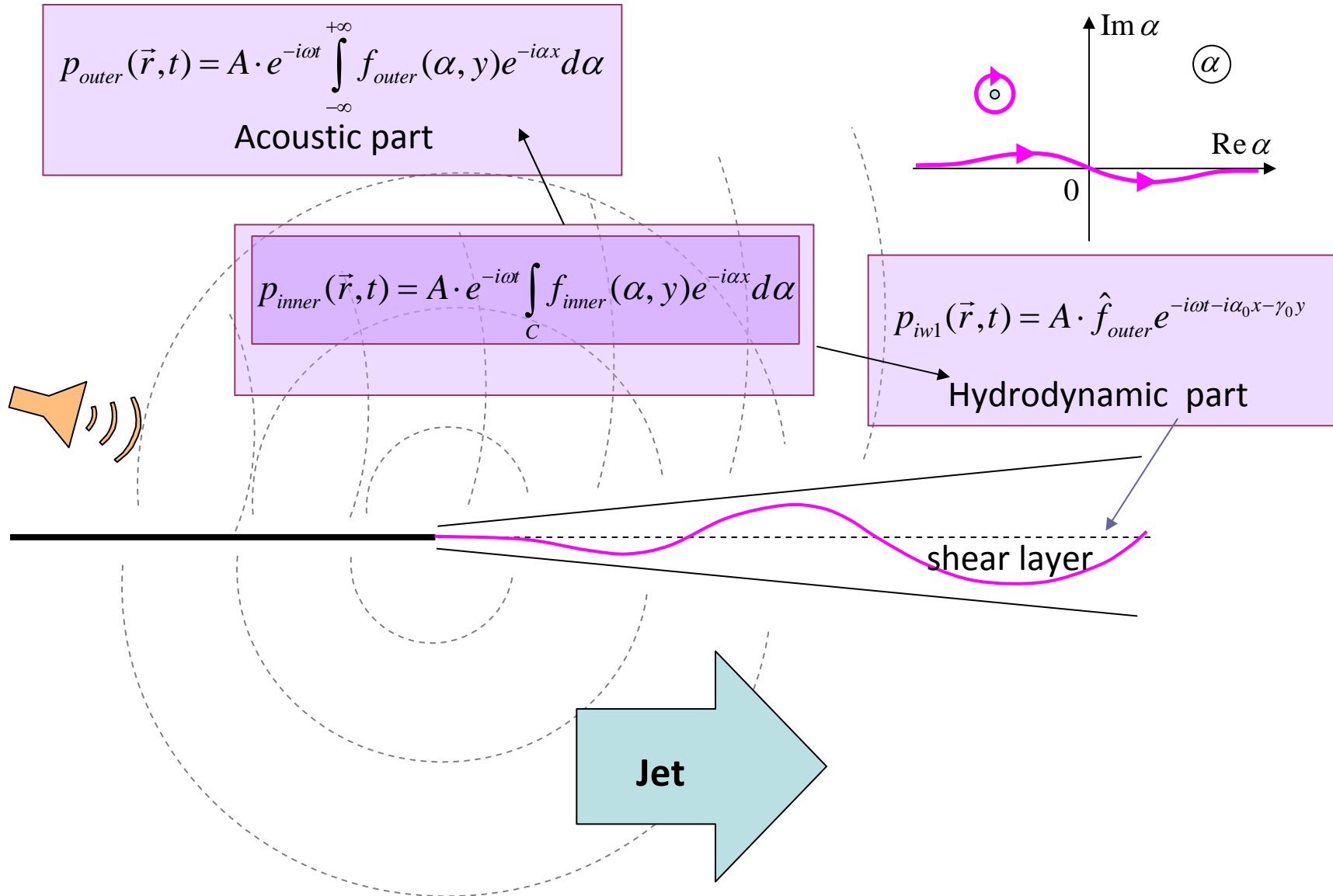
$$p_{iw2}(\vec{r}, t) = B \cdot \hat{f}_{inner} e^{-i\omega t - i\alpha_0 x - \gamma_0 y}$$

Hydrodynamic part



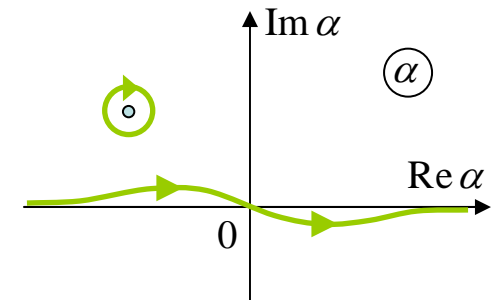
Full solution contains the incident wave, diffraction field and instability wave which together satisfy the Kutta condition near the edge.

Therefore the instability wave initial amplitude is determined by the incident wave properties only.



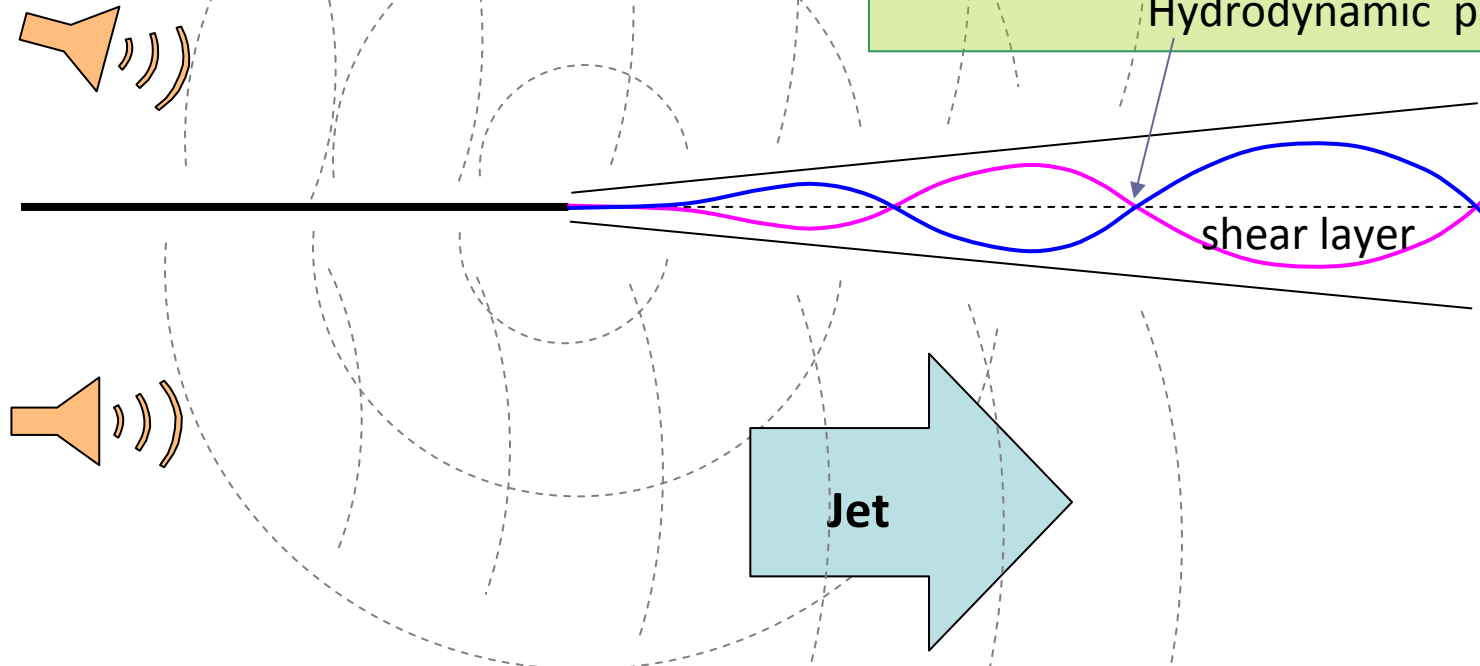
$$p(\vec{r}, t) = e^{-i\omega t} \int_{-\infty}^{+\infty} (A \cdot f_{outer}(\alpha, y) + B \cdot f_{inner}(\alpha, y)) e^{-i\alpha x} d\alpha$$

Acoustic part



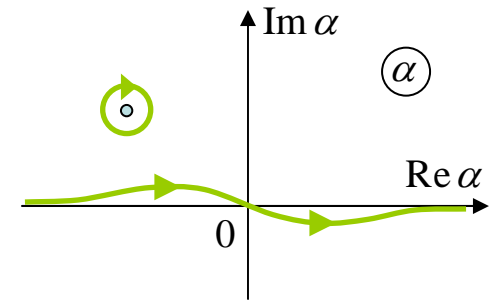
$$p_{iw}(\vec{r}, t) = (A \cdot \hat{f}_{outer} + B \cdot \hat{f}_{inner}) e^{-i\omega t - i\alpha_0 x - \gamma_0 y}$$

Hydrodynamic part



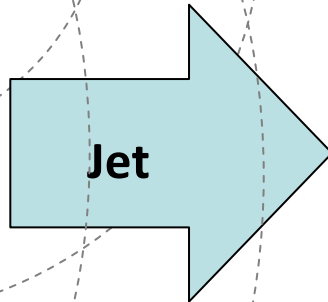
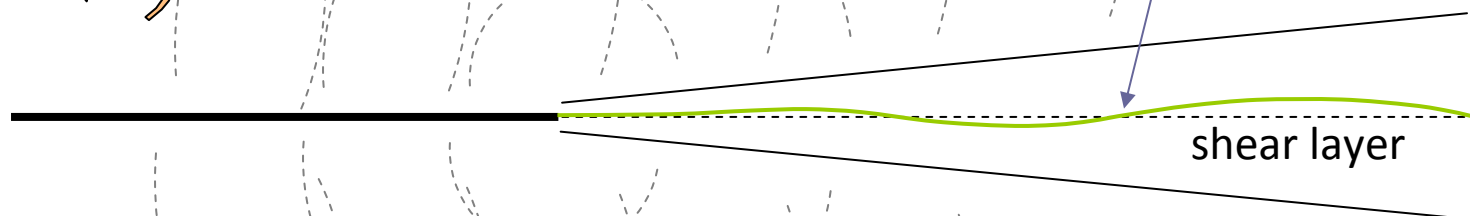
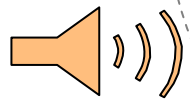
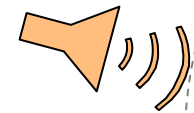
$$p(\vec{r}, t) = e^{-i\omega t} \int_{-\infty}^{+\infty} (A \cdot f_{outer}(\alpha, y) + B \cdot f_{inner}(\alpha, y)) e^{-i\alpha x} d\alpha$$

Acoustic part $\neq 0$

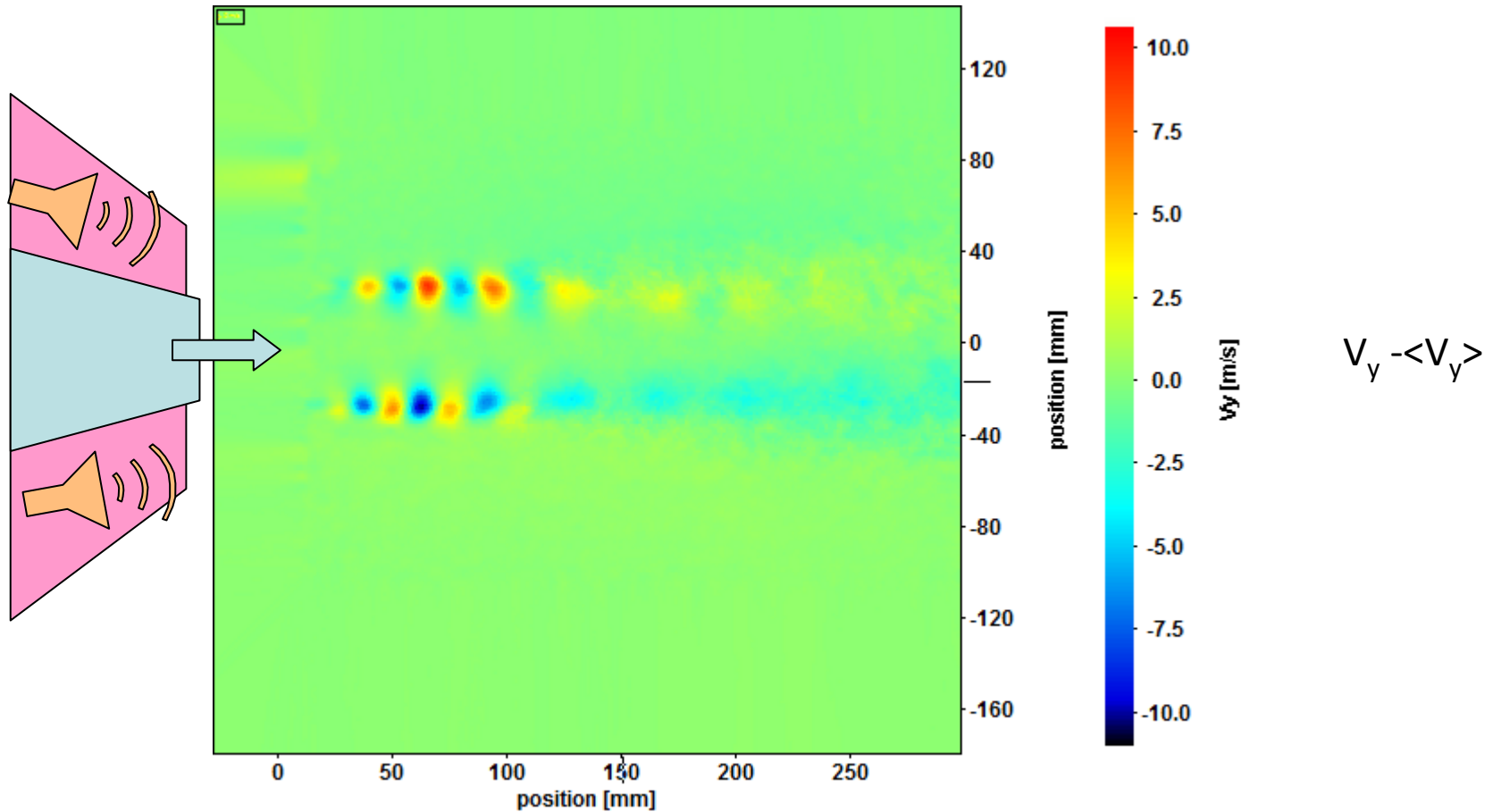


$$p_{iw}(\vec{r}, t) = 0, \quad A = -B \cdot \hat{f}_{inner} / \hat{f}_{outer}$$

Hydrodynamic part = 0

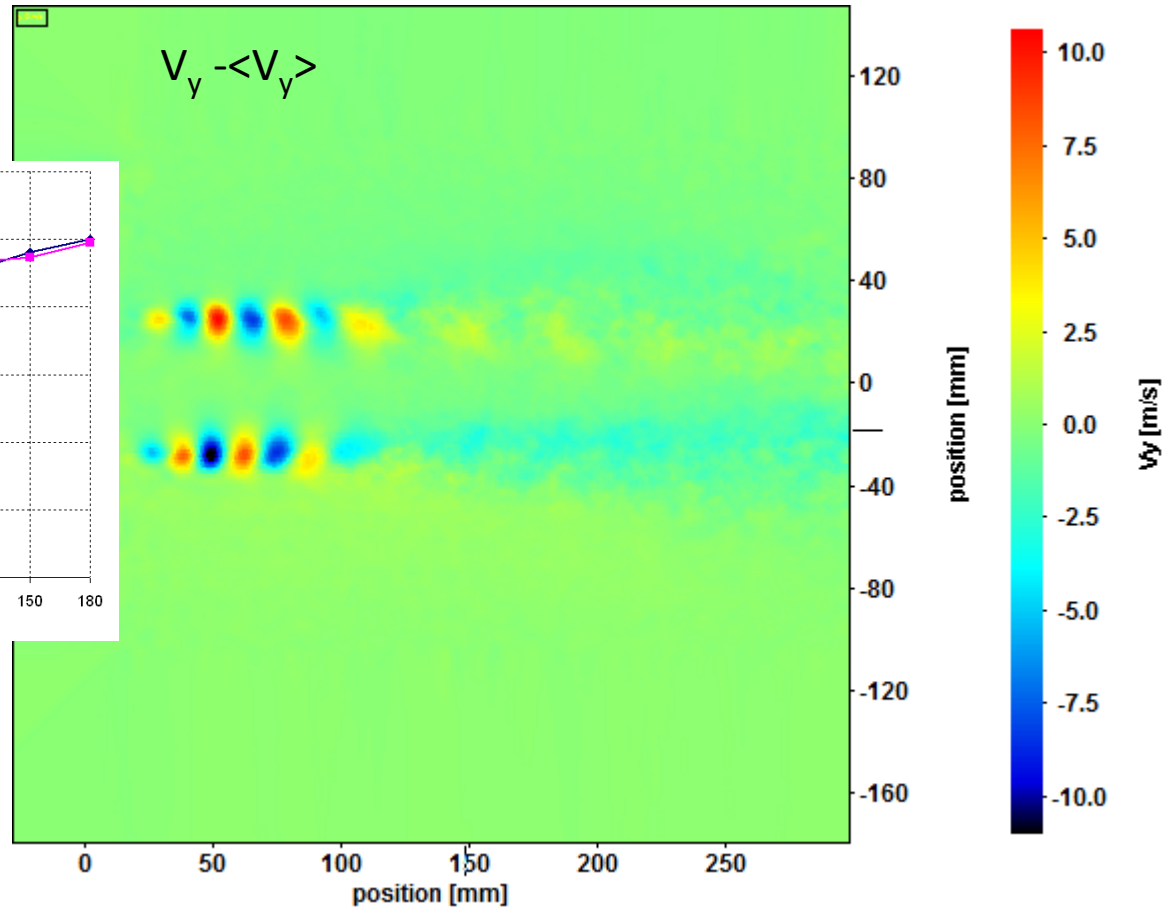
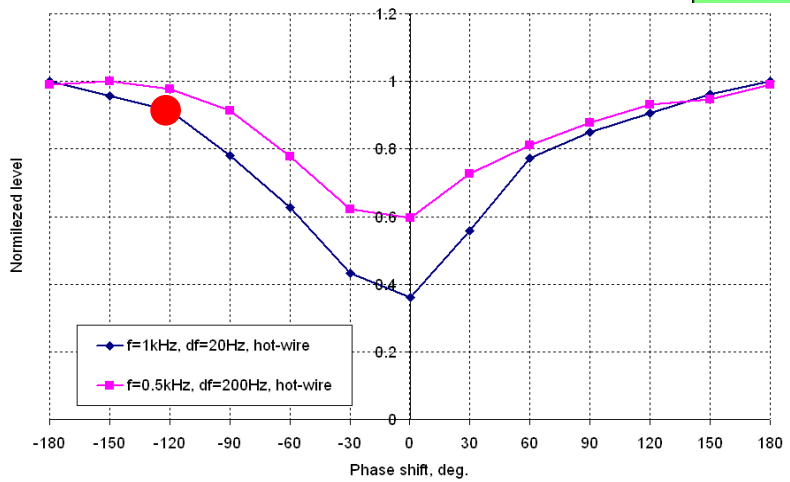


PIV measurements , $f_{exc} = f_{samp} = 1\text{kHz}$



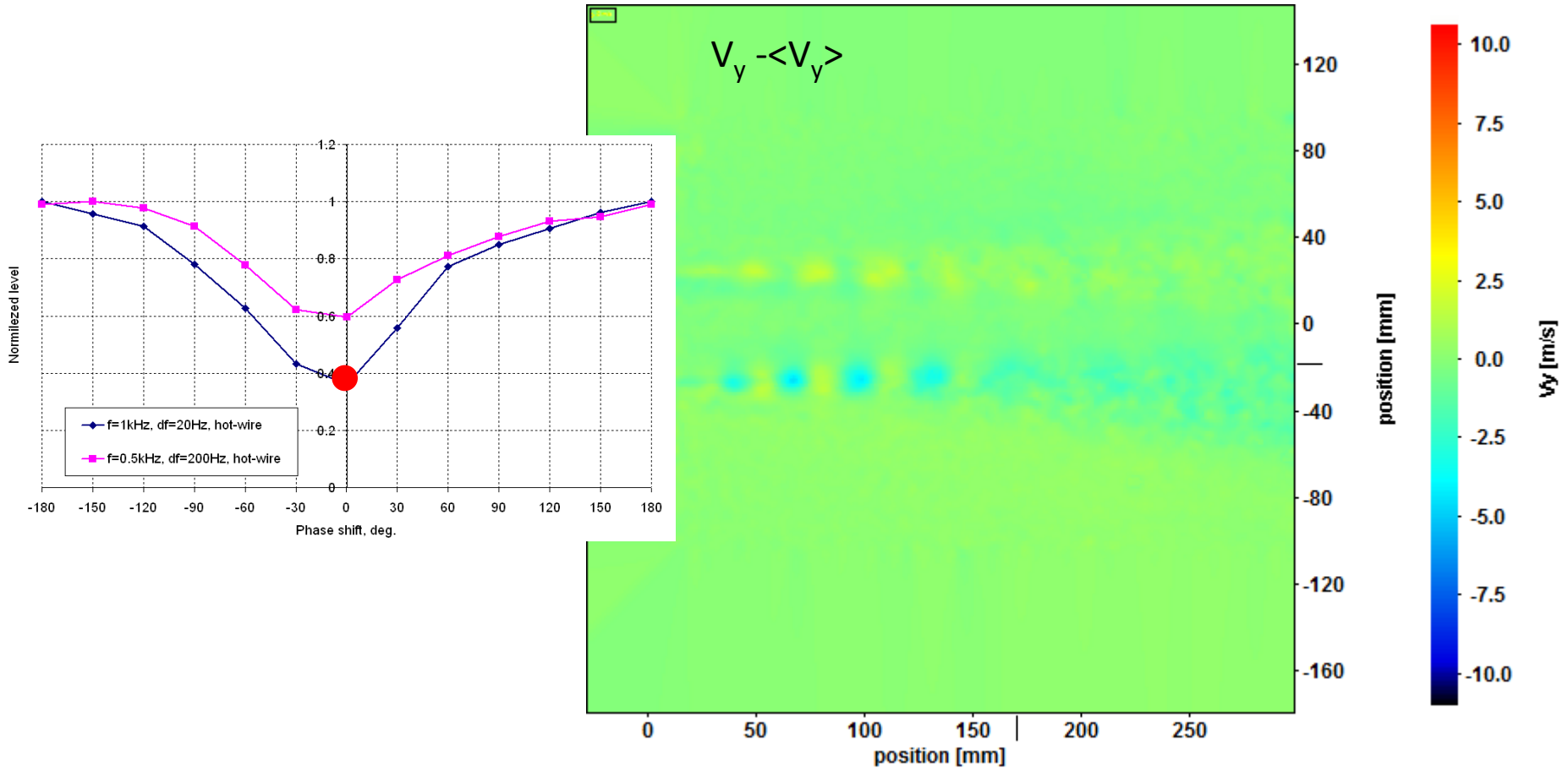
Outer source

PIV measurements , $f_{exc} = f_{samp} = 1\text{kHz}$



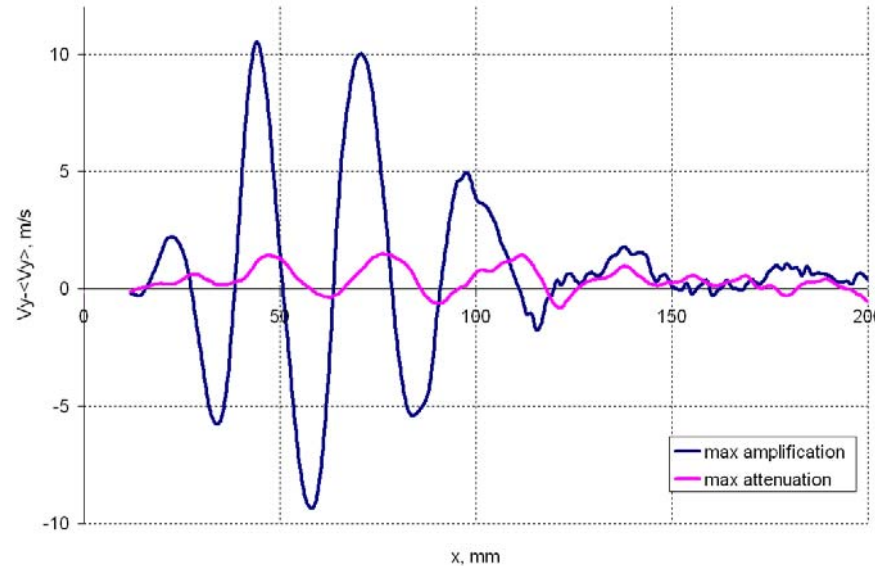
$$\Delta \phi = -180^\circ$$

PIV measurements , $f_{exc} = f_{samp} = 1\text{kHz}$



$$\Delta \phi = -60^\circ$$

PIV measurements , $f_{\text{exc}} = f_{\text{samp}} = 1\text{kHz}$



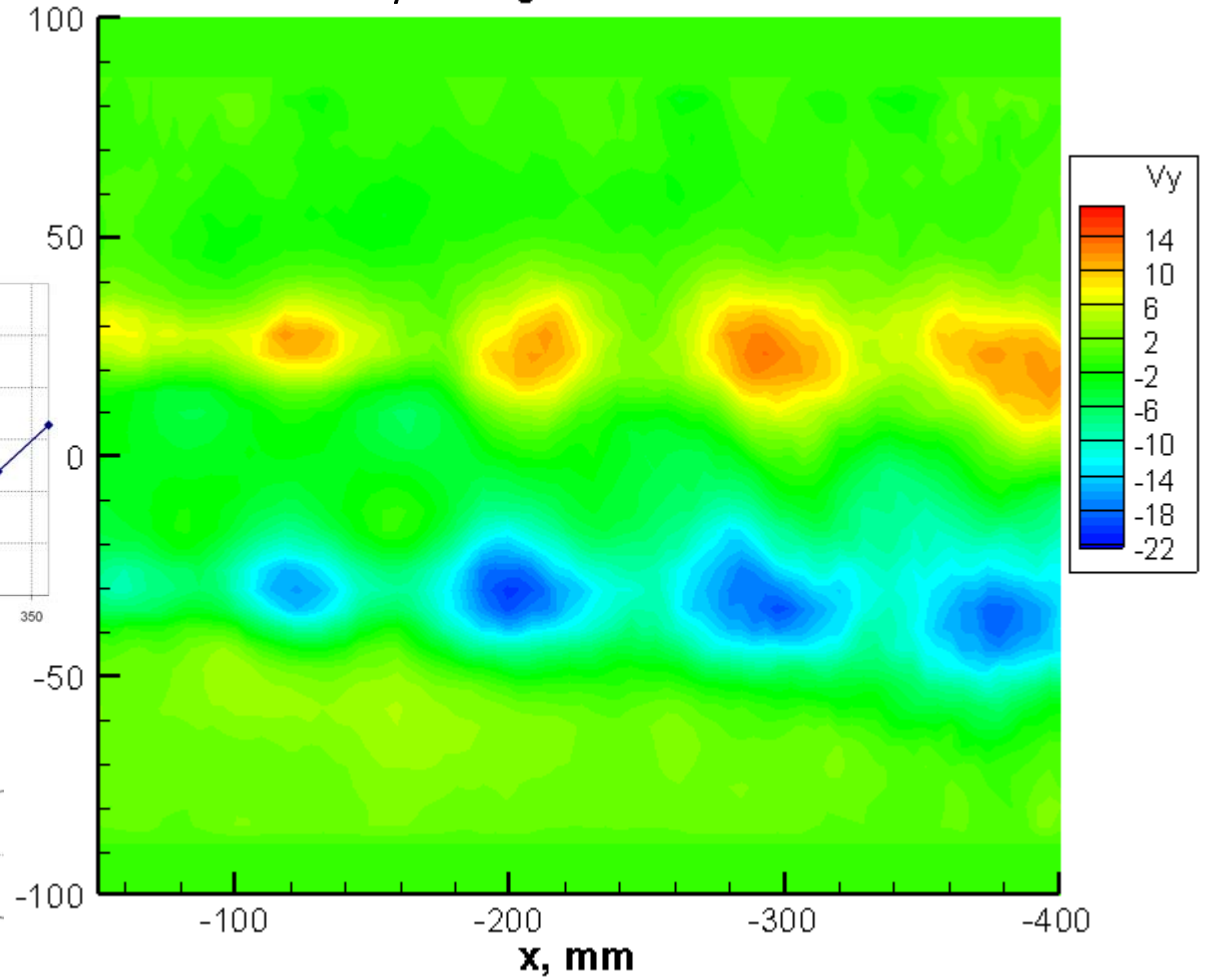
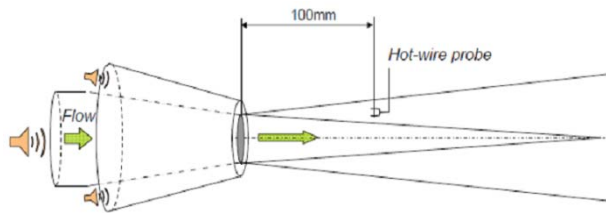
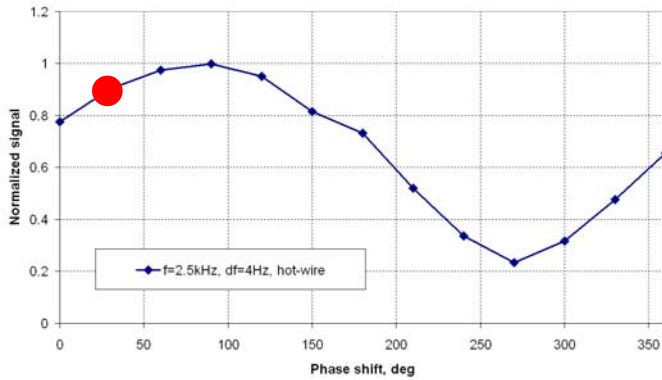
Profile of $V_y - \langle V_y \rangle$ along the lip-line

Jet velocity 280 m/s

Measurements by TR PIV, $f_{exc} = f_{samp} = 2.5 \text{ k} \Gamma \text{ ц}$

$\Delta \phi = 30 \text{ deg}$

Measurements by hot-wire

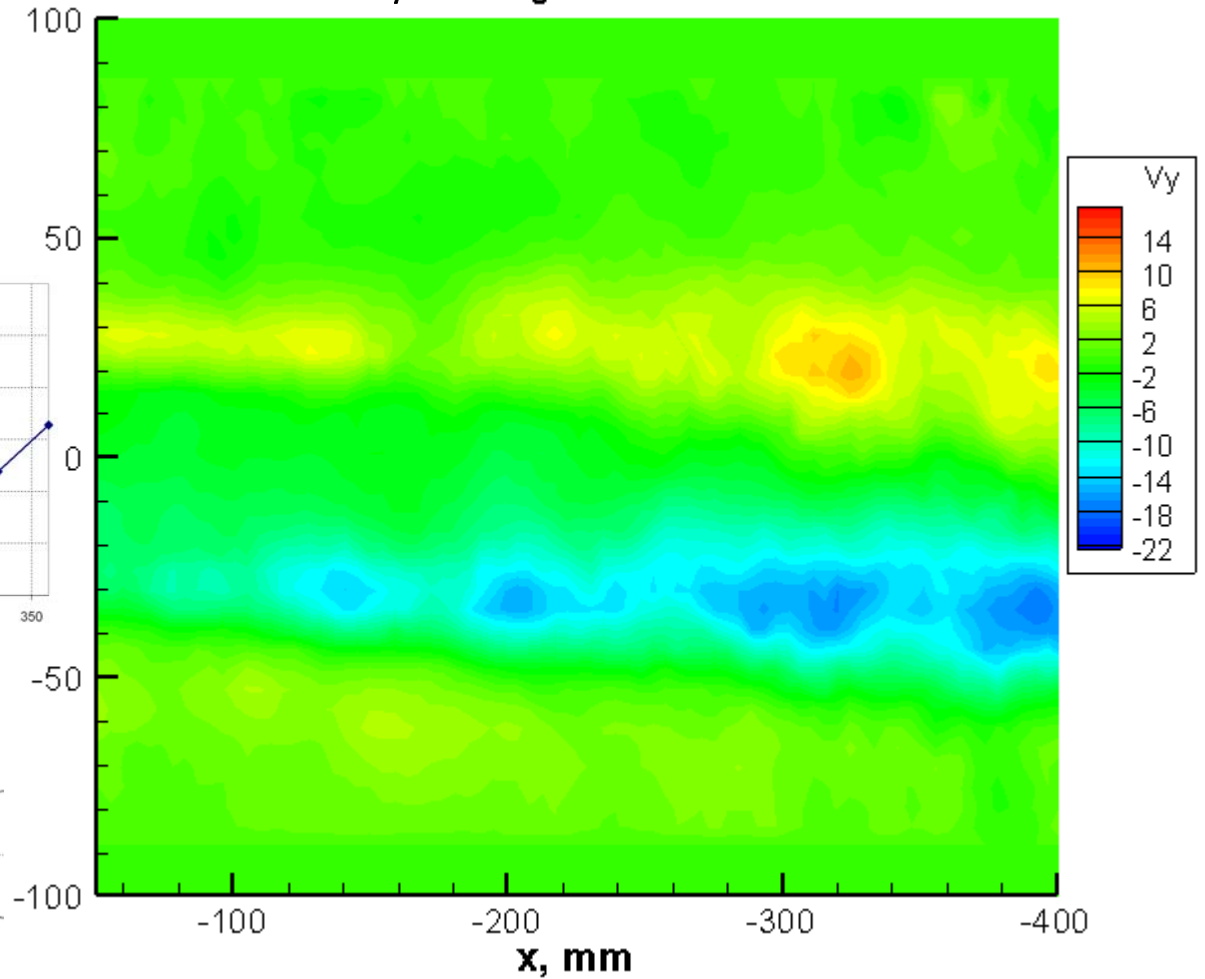
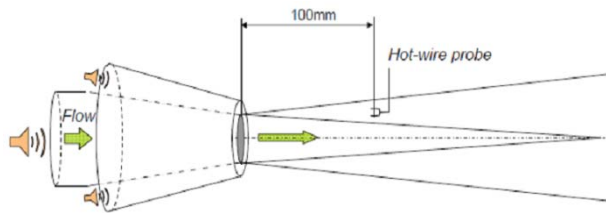
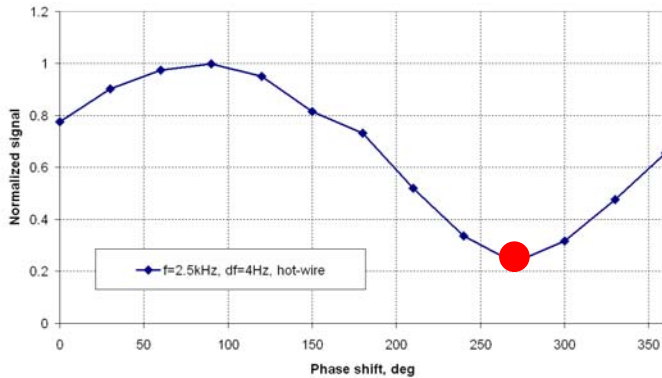


Jet velocity 280 m/s

Measurements by TR PIV, $f_{exc} = f_{samp} = 2.5 \text{ k} \Gamma \text{ ц}$

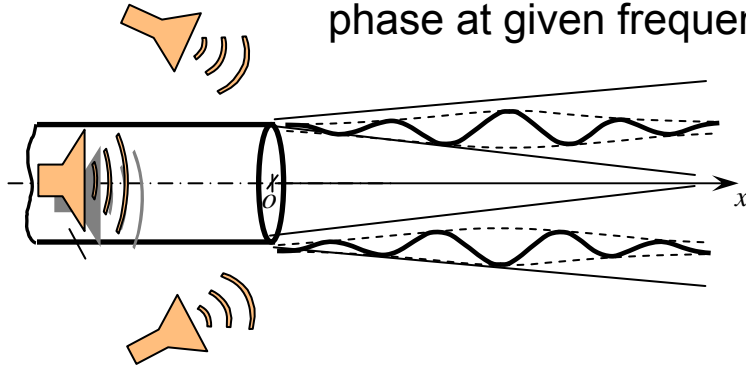
$\Delta \phi = 270 \text{ deg}$

Measurements by hot-wire

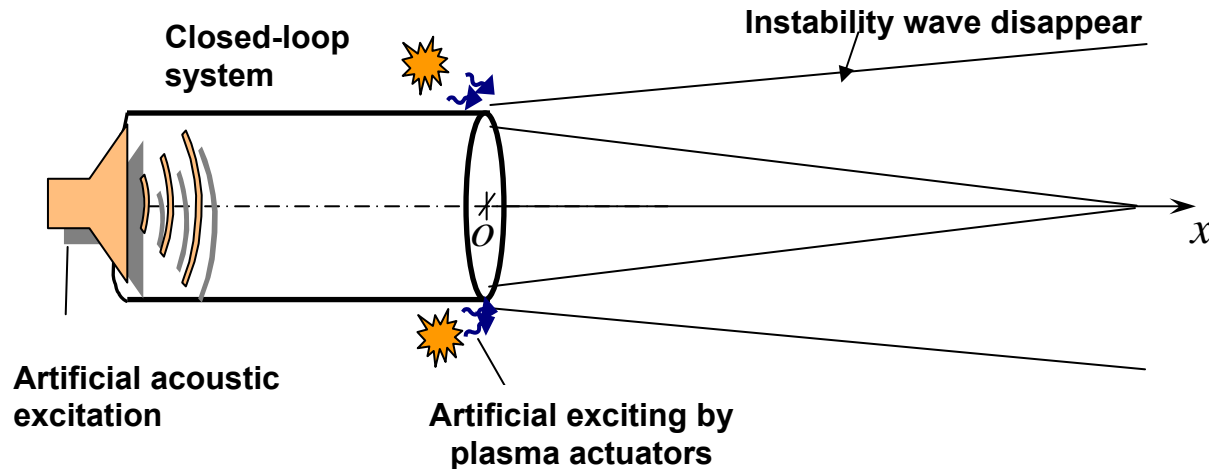
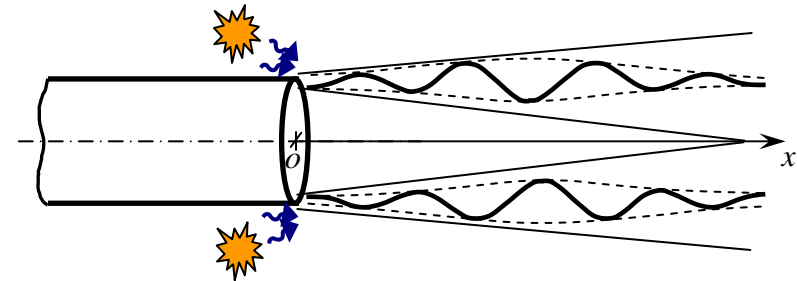


Plasma actuator for IW suppression

Artificial acoustic excitation characterized by amplitude and phase at given frequency



Artificial exciting by plasma actuators



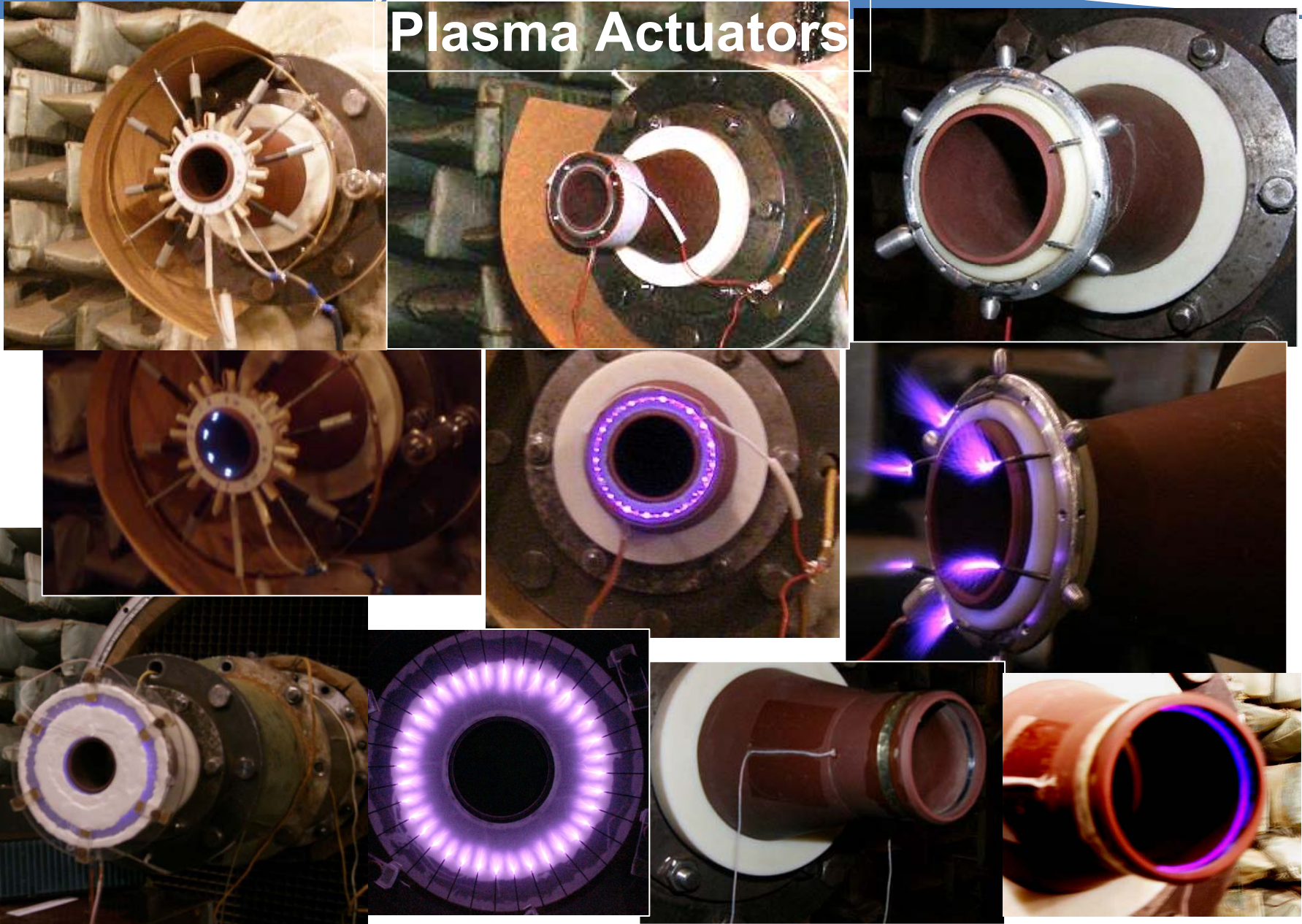
Witoszynski ceramic nozzles



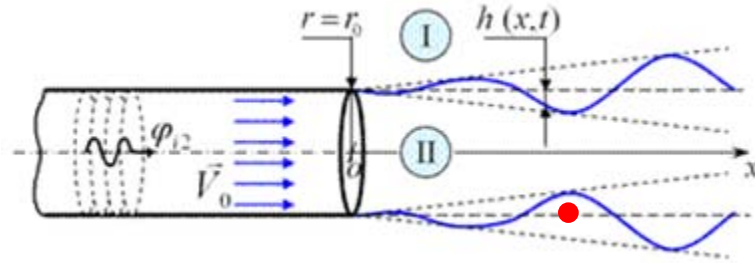
$$r(x) = \frac{r_2}{\sqrt{1 - \left(1 - \left(\frac{r_2}{r_1}\right)^2\right) \frac{\left(1 - \frac{x^2}{L^2}\right)^2}{\left(1 + \frac{x^2}{L^2}\right)^3}}}$$



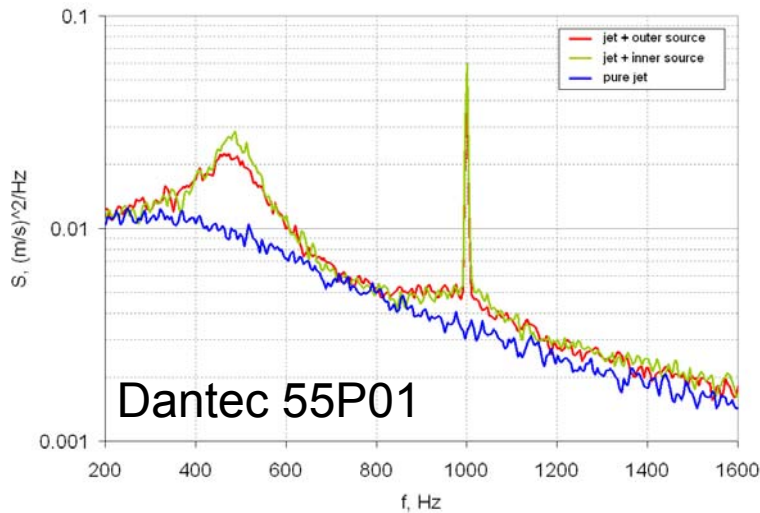
Plasma Actuators



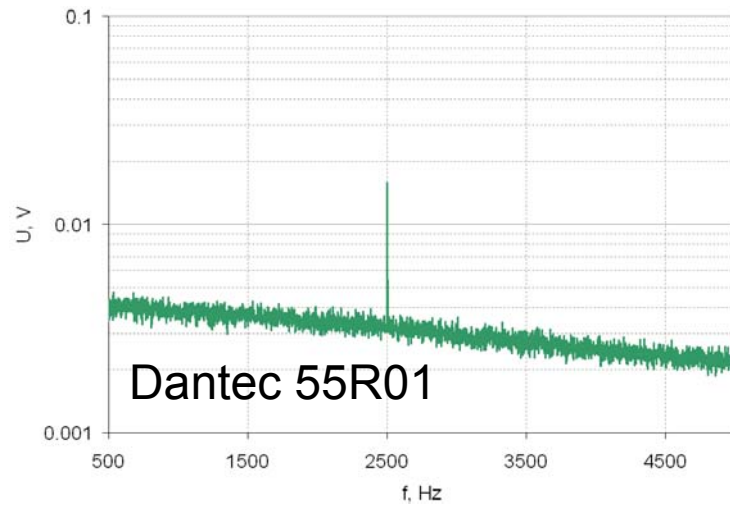
Hot-wire measurements



V=50 m/s, at f=1kHz

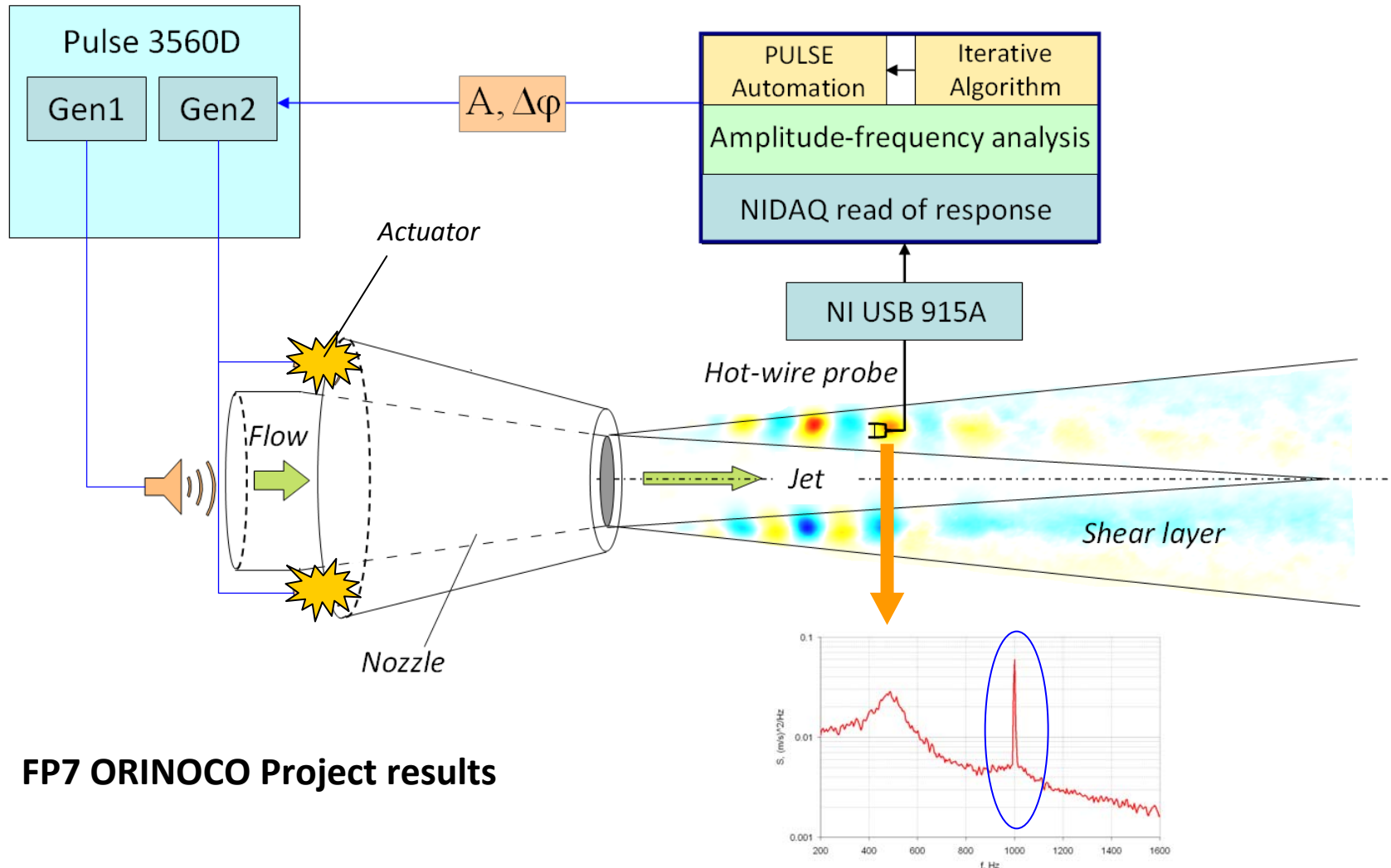


V=280 m/s, at f=2.5kHz



Closed loop AIW control system

Kopiev et al. (2013, 2014)



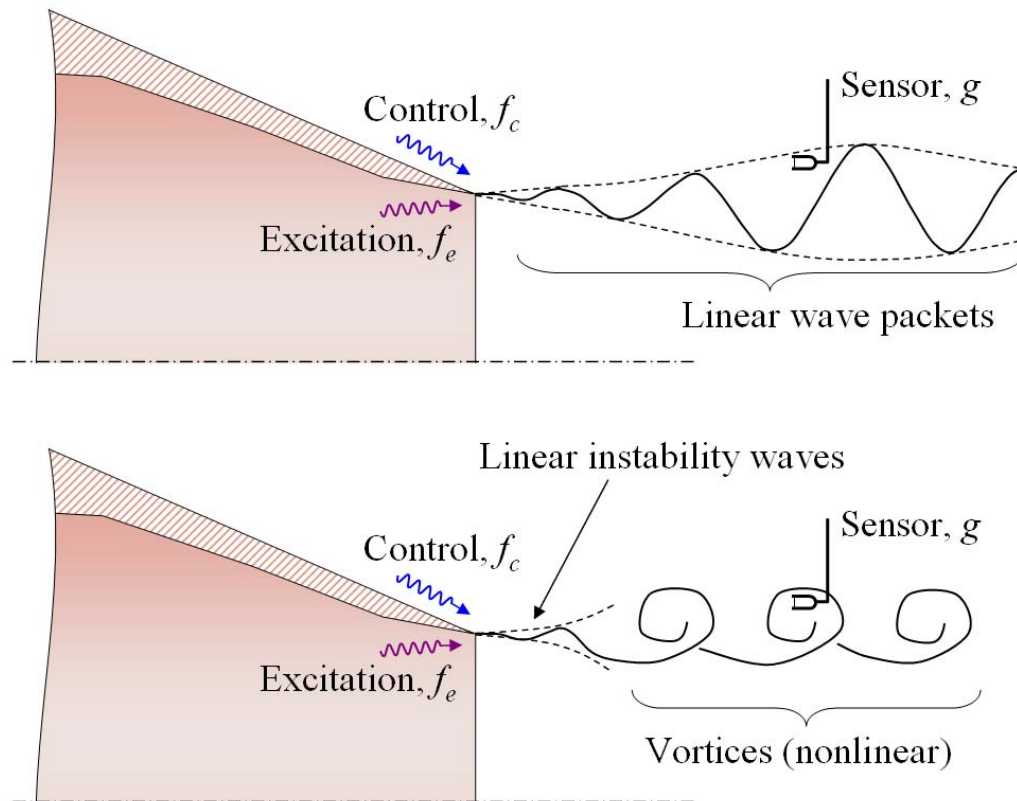
FP7 ORINOCO Project results

Outline

- Introduction
- Artificial instability waves (AIW) , AIW control strategy
- **NIW control idea, Overview of LES-results**
- Data analysis in the jet shear layer
- Data analysis in the jet near field
- Experimental data
- NIW Control strategy
- Conclusion

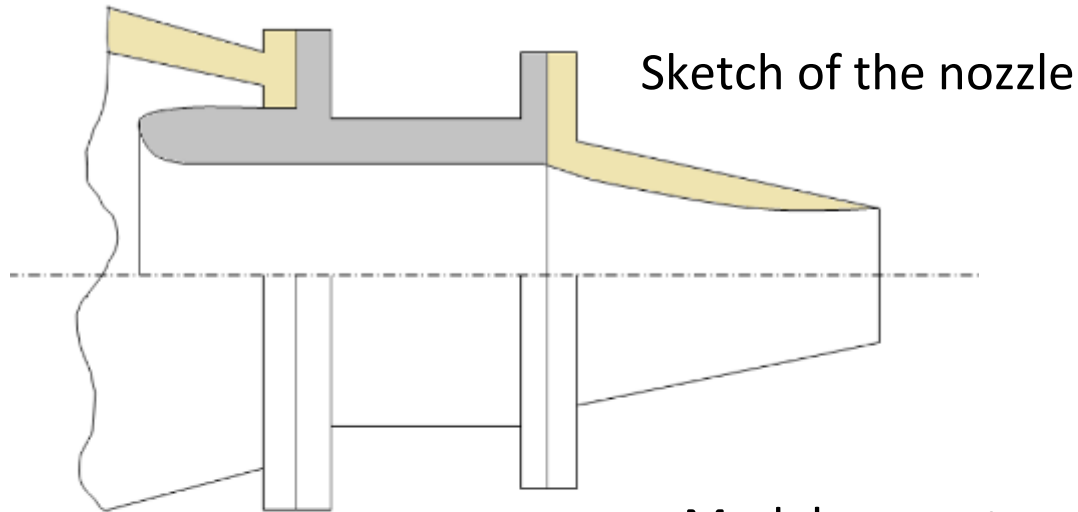
How to control Natural Instability waves (NIW)?

Instabilities in excited jet: nonlinear and linear regimes



Overview of LES-results

Profiled TsAGI nozzle



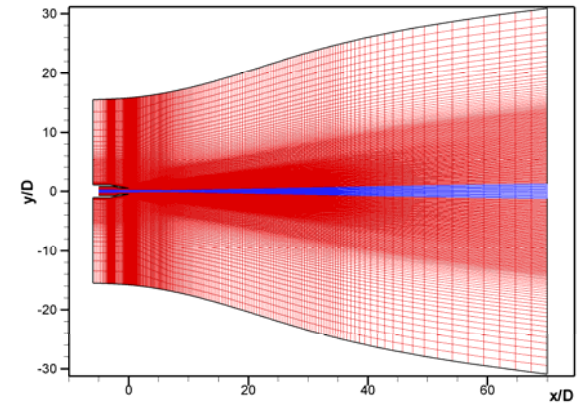
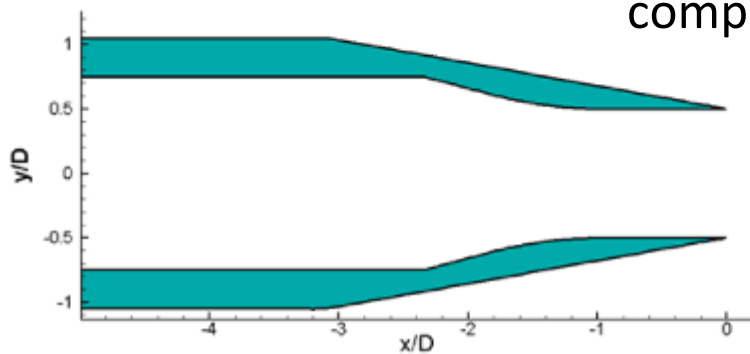
Operating conditions

$$V_{\text{jet}} = 280 \text{ m/s}$$

$$D = 0.04 \text{ m}$$

$$T^* = 290 \text{ K}$$

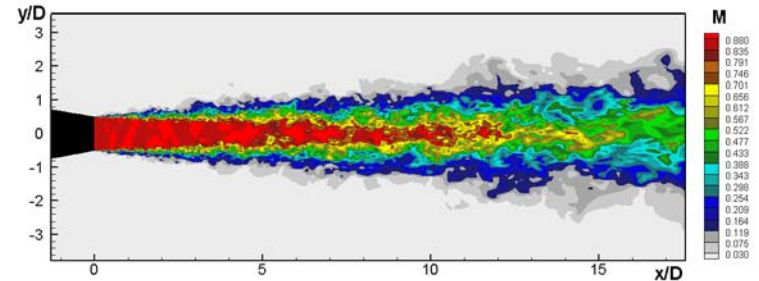
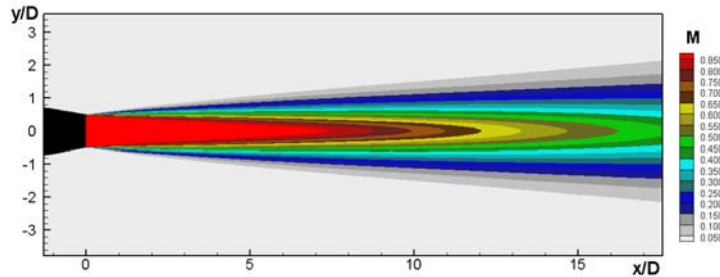
Model geometry and computational mesh



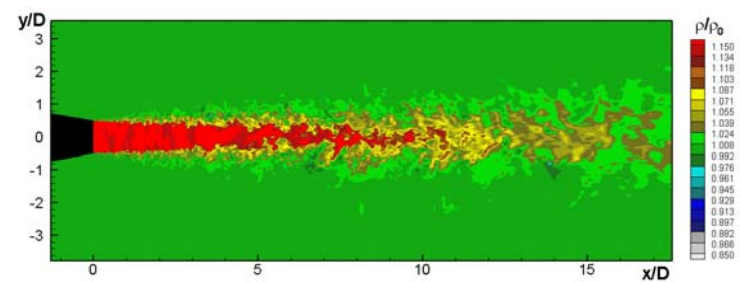
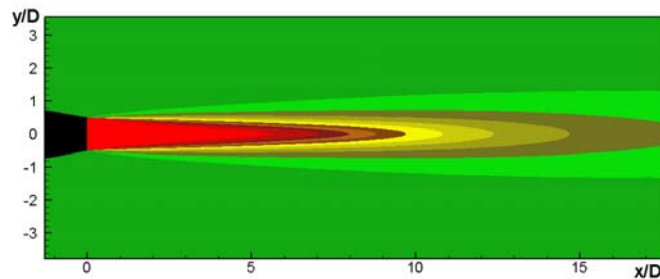
Simultaneous and averaged fields in symmetry plane

LES simulation by M.Shur and M.Strelets

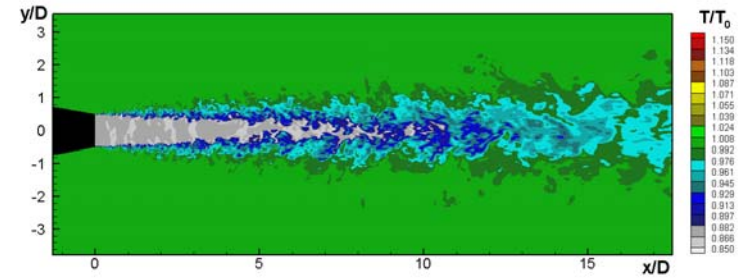
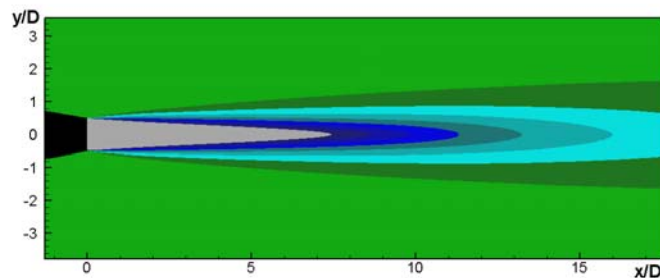
Mach number



Density

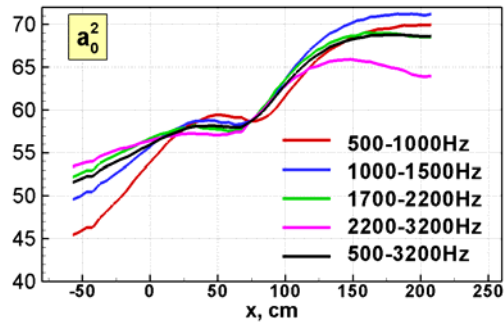


Temperature

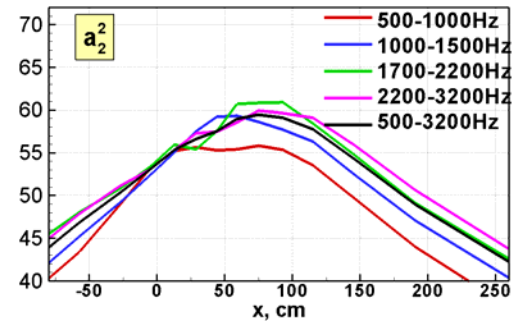
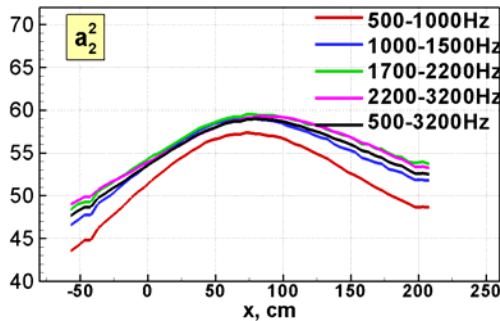
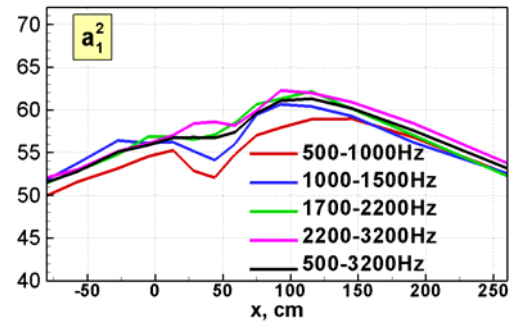
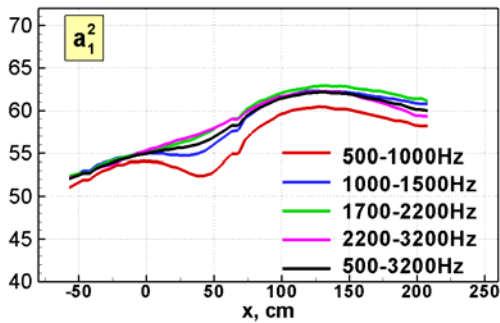
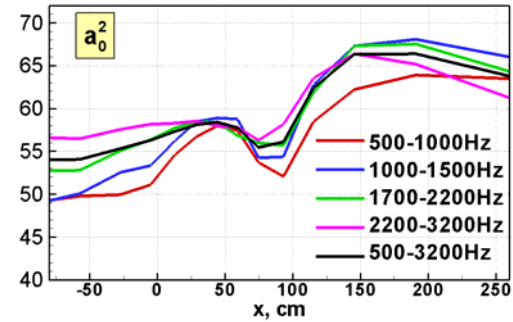


Validation of LES data in far acoustic field

Experiment

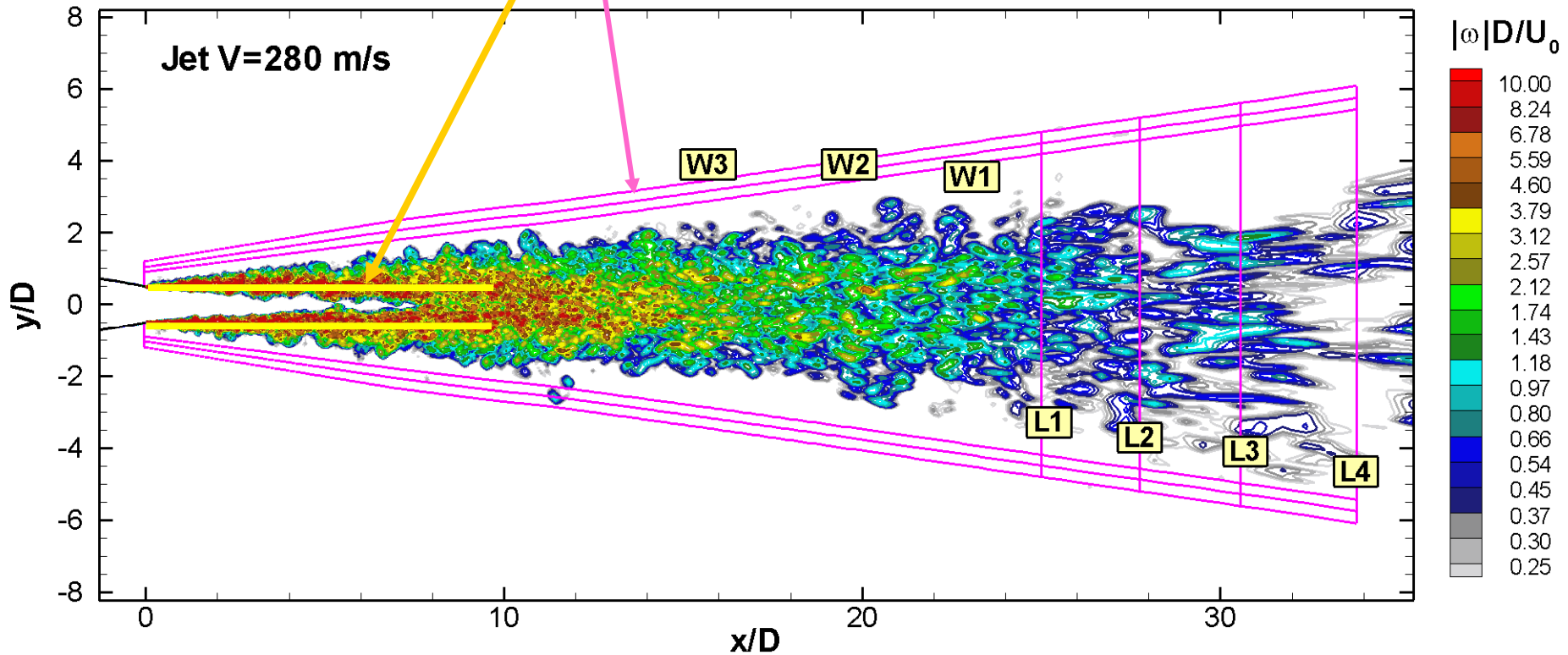


Simulation



Surfaced with saved pulsations time histories

1. Cylindrical lip-line surface
2. Control FWH surfaces in the jet near field

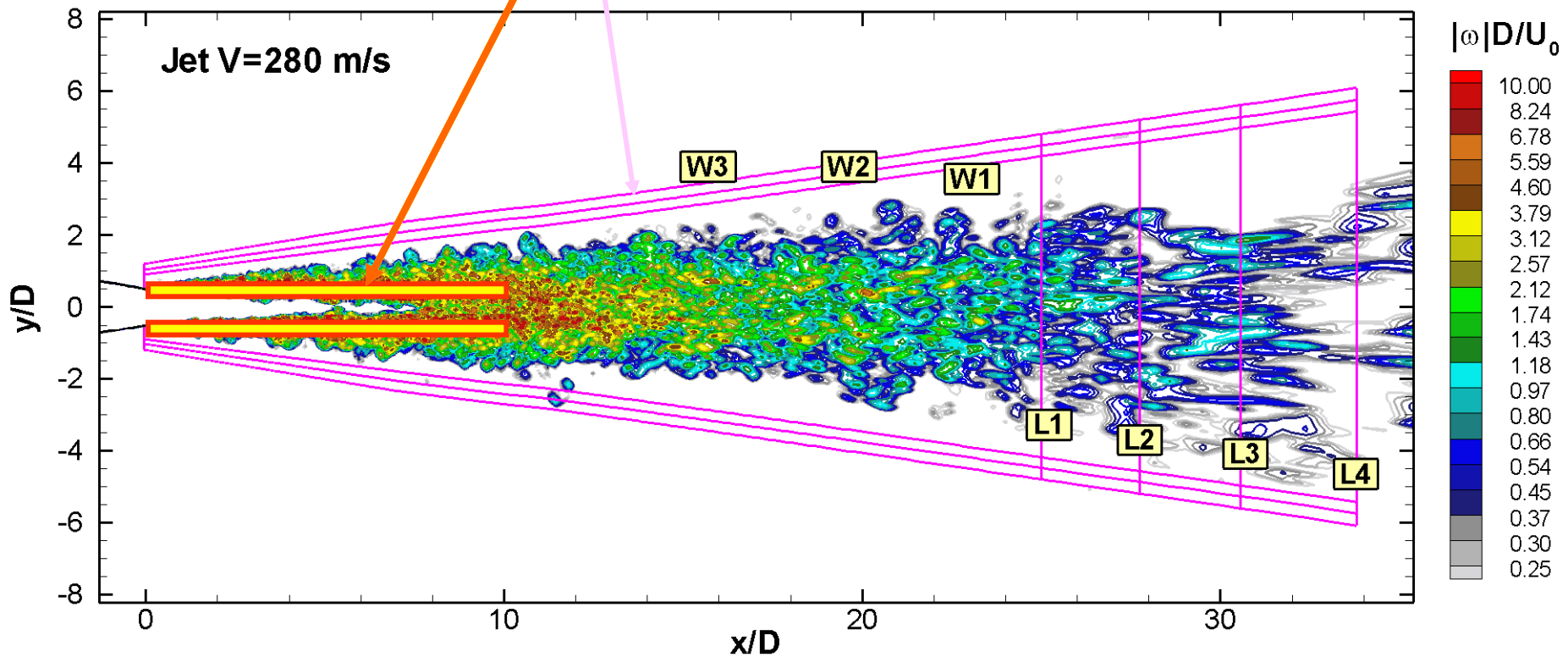


Outline

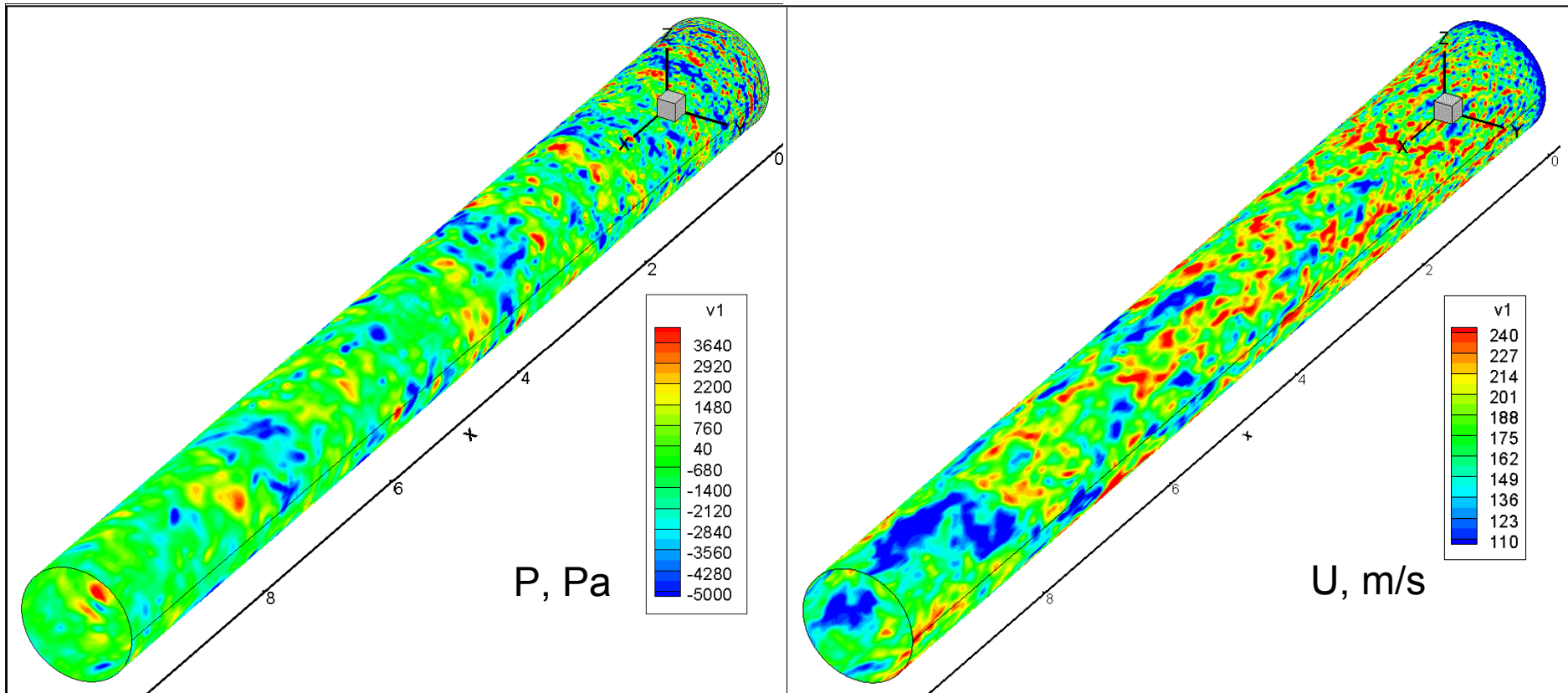
- Introduction
- Artificial instability waves (AIW) , AIW control strategy
- NIW control idea, Overview of LES-results,
- **Data analysis in the jet shear layer**
- Data analysis in the jet near field
- Experimental data
- NIW Control strategy
- Conclusion

Surfaced with saved pulsations time histories

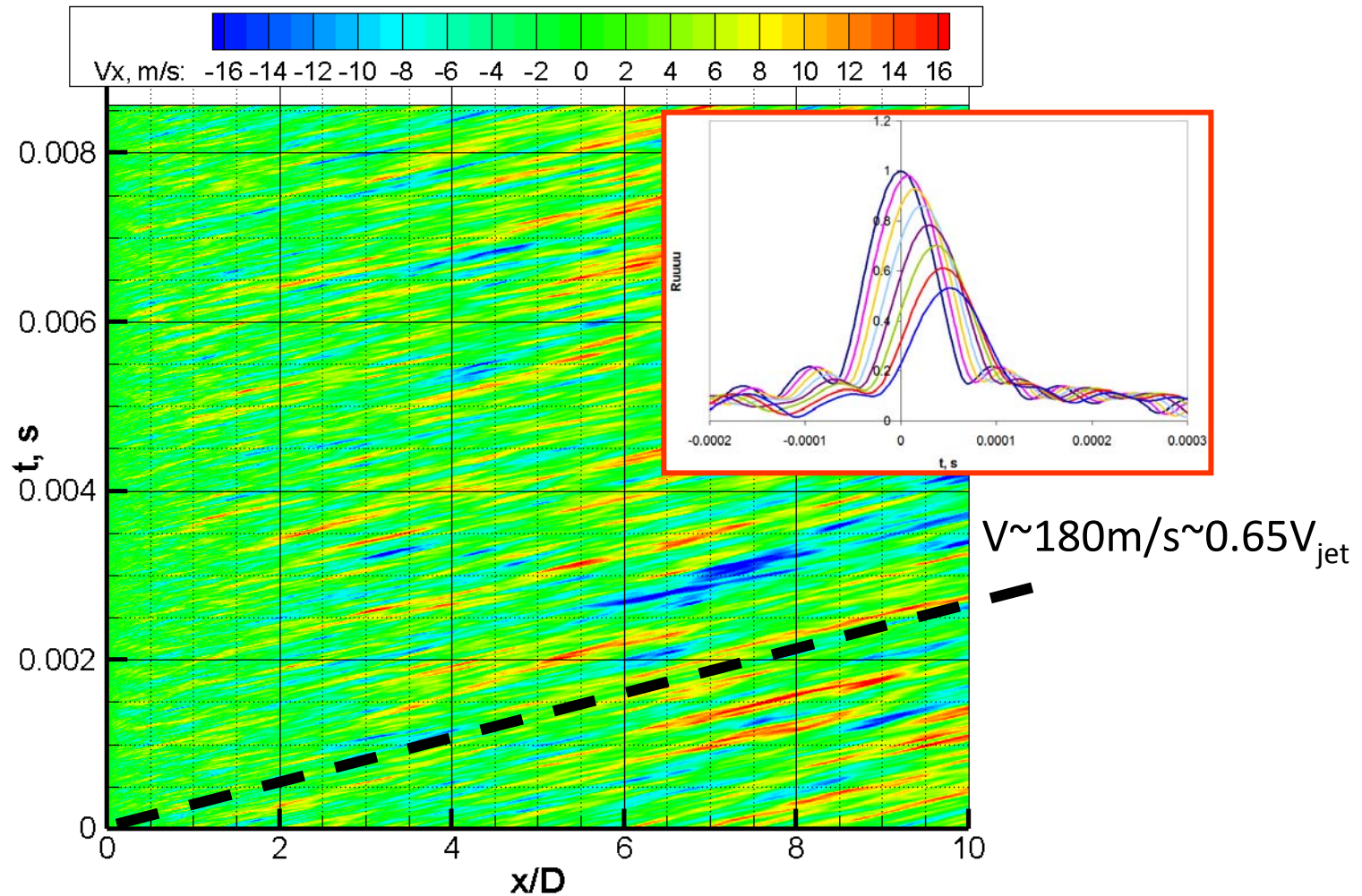
1. Cylindrical lip-line surface
2. Control FWH surfaces in the jet near field



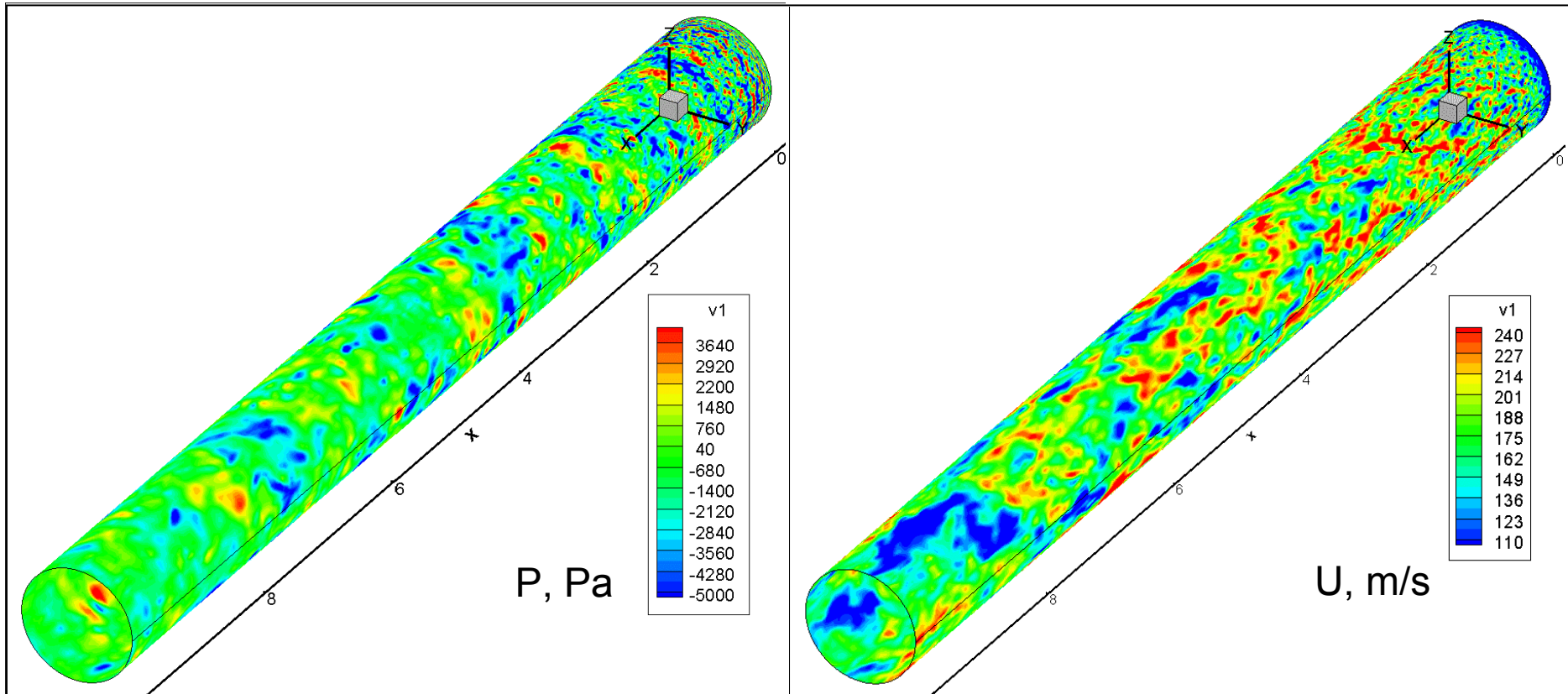
Time evolution of pressure and axial velocity pulsations



Time evolution of pressure and axial velocity pulsations

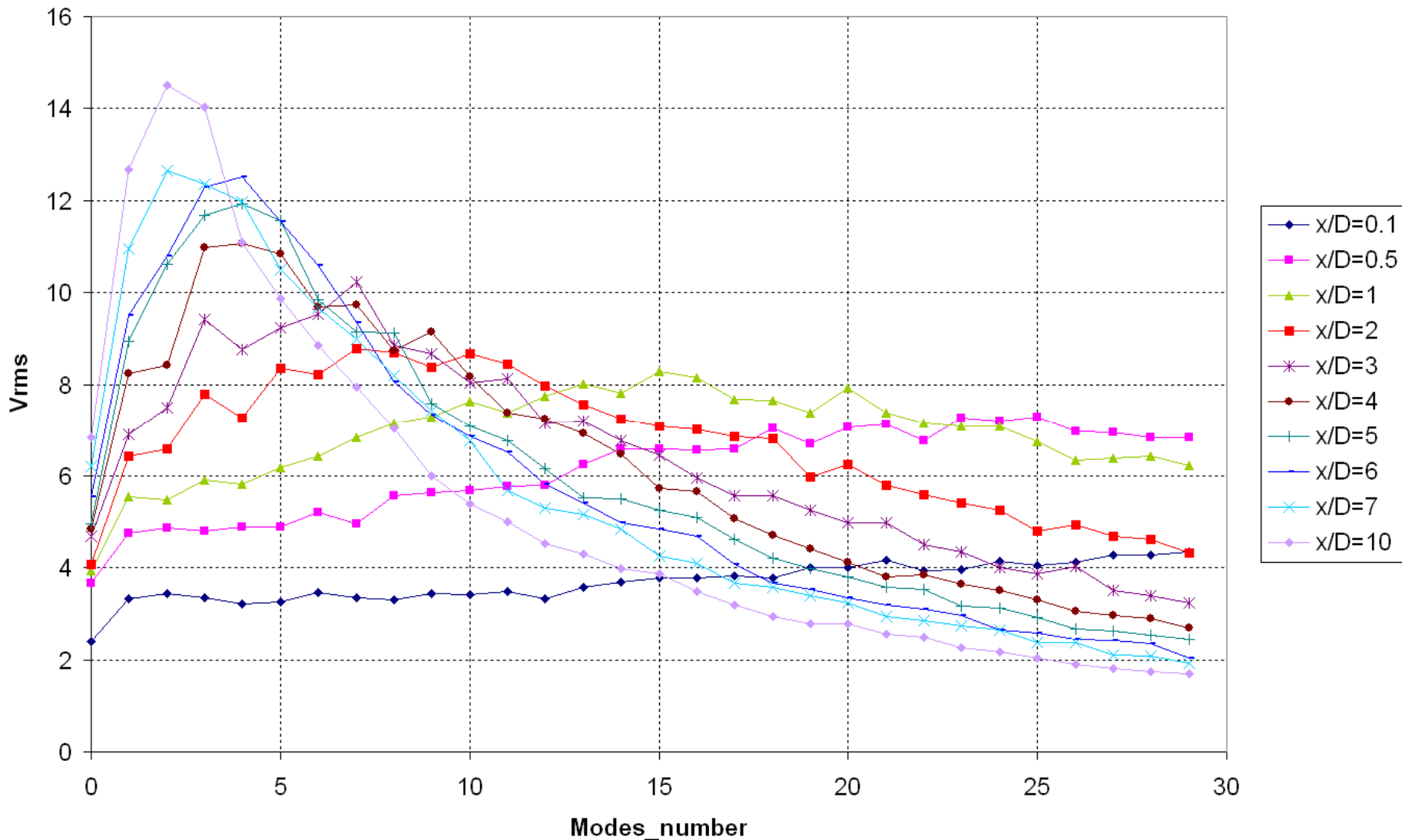


Time evolution of pressure and axial velocity pulsations

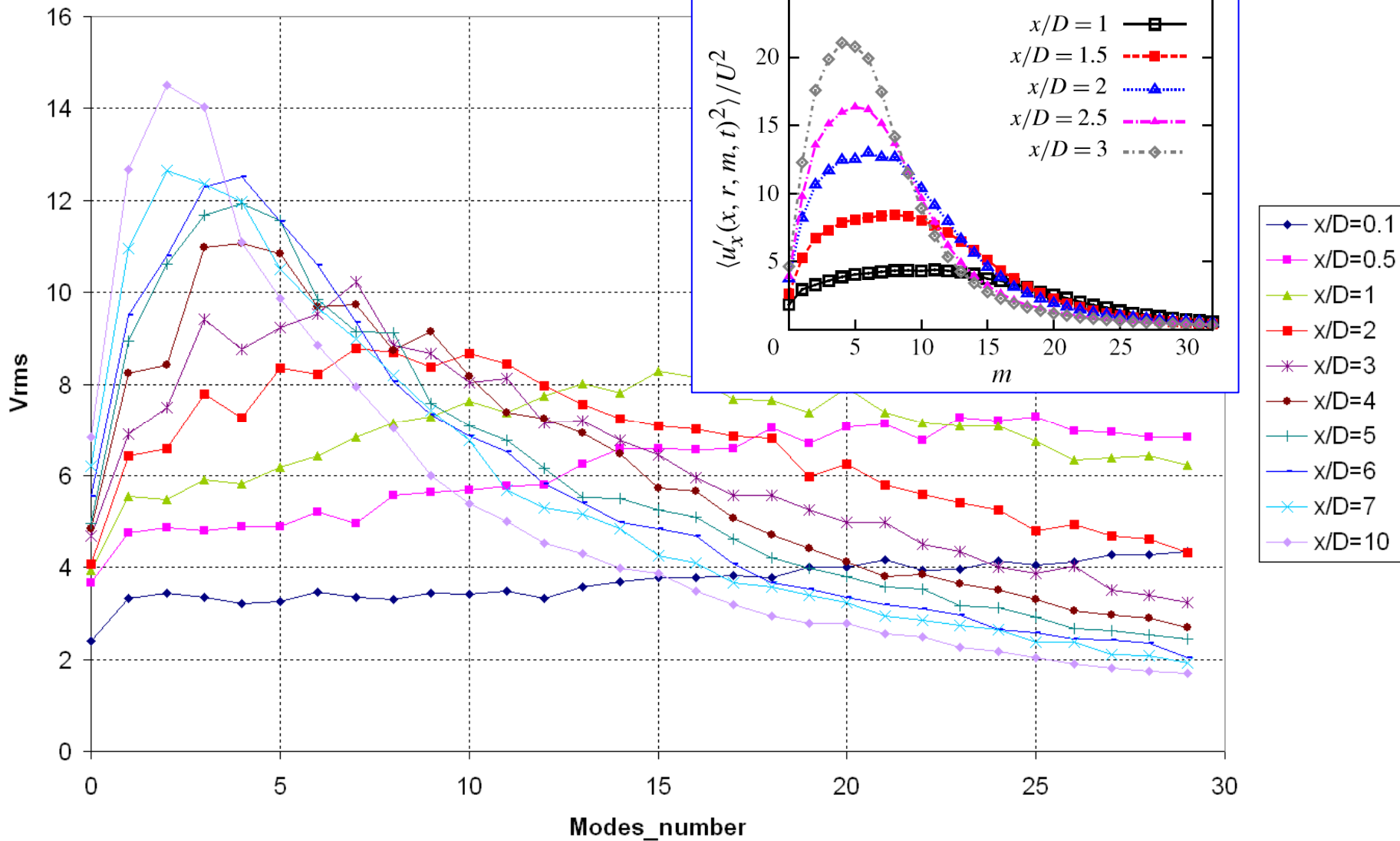


$$f(x, \theta, t) = \sum_{n=0}^N \left(f_n^{\cos}(x, t) \cos n\theta + f_n^{\sin}(x, t) \sin n\theta \right)$$

Modal content of velocity pulsations



Modal content of velocity fluctuations (a) $(\times 10^{-4})$ Cavalieri A.V. et al. (2013)

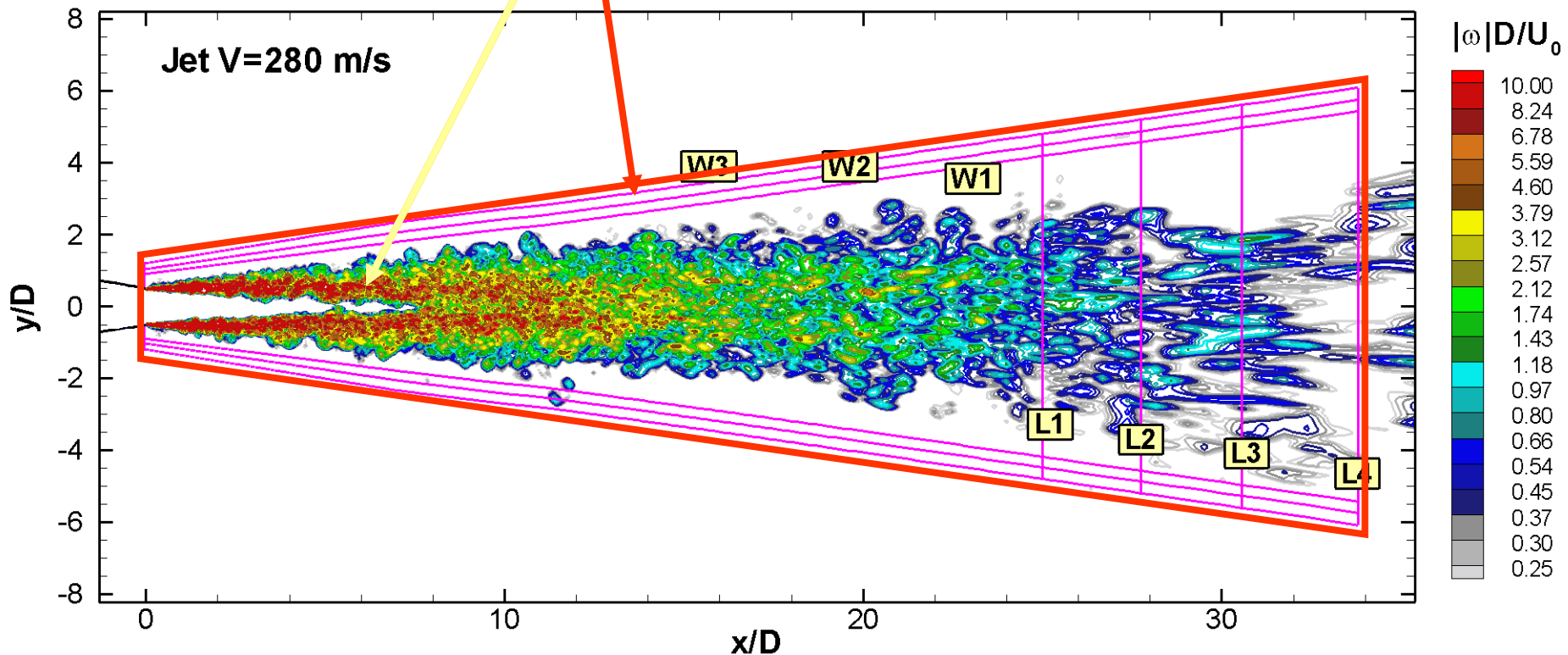


Outline

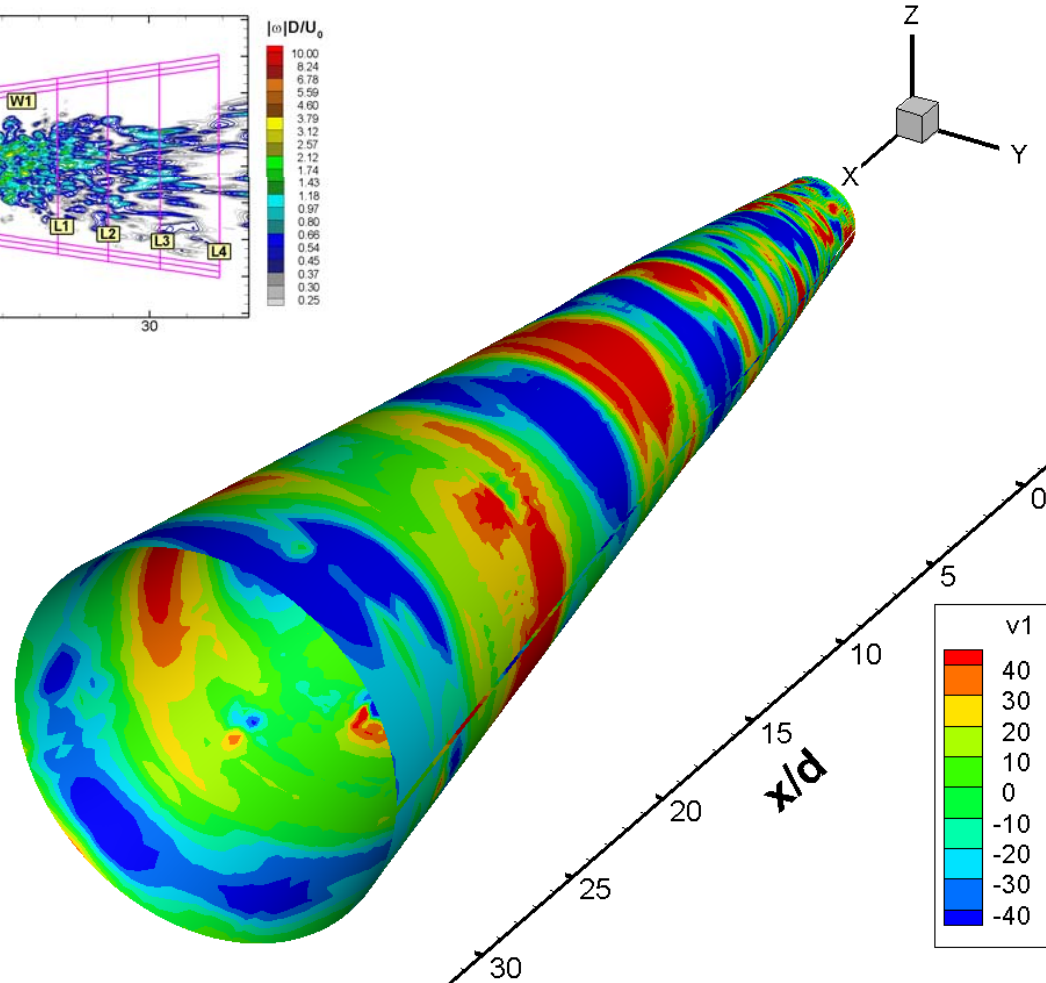
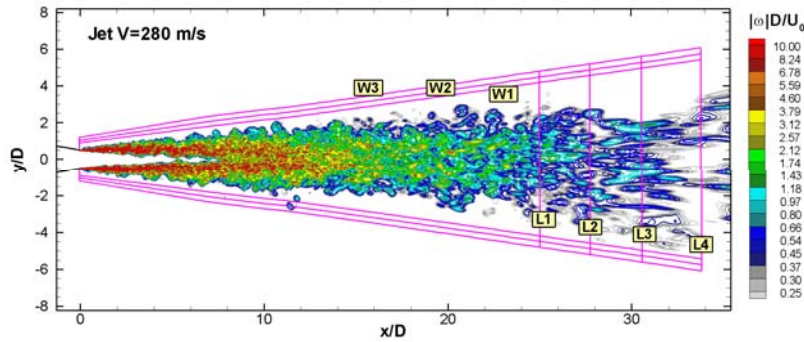
- Introduction
- Artificial instability waves (AIW) , AIW control strategy
- NIW control idea, Overview of LES-results,
- Data analysis in the jet shear layer
- **Data analysis in the jet near field**
- Experimental data
- NIW Control strategy
- Conclusion

Surfaced with saved pulsations time histories

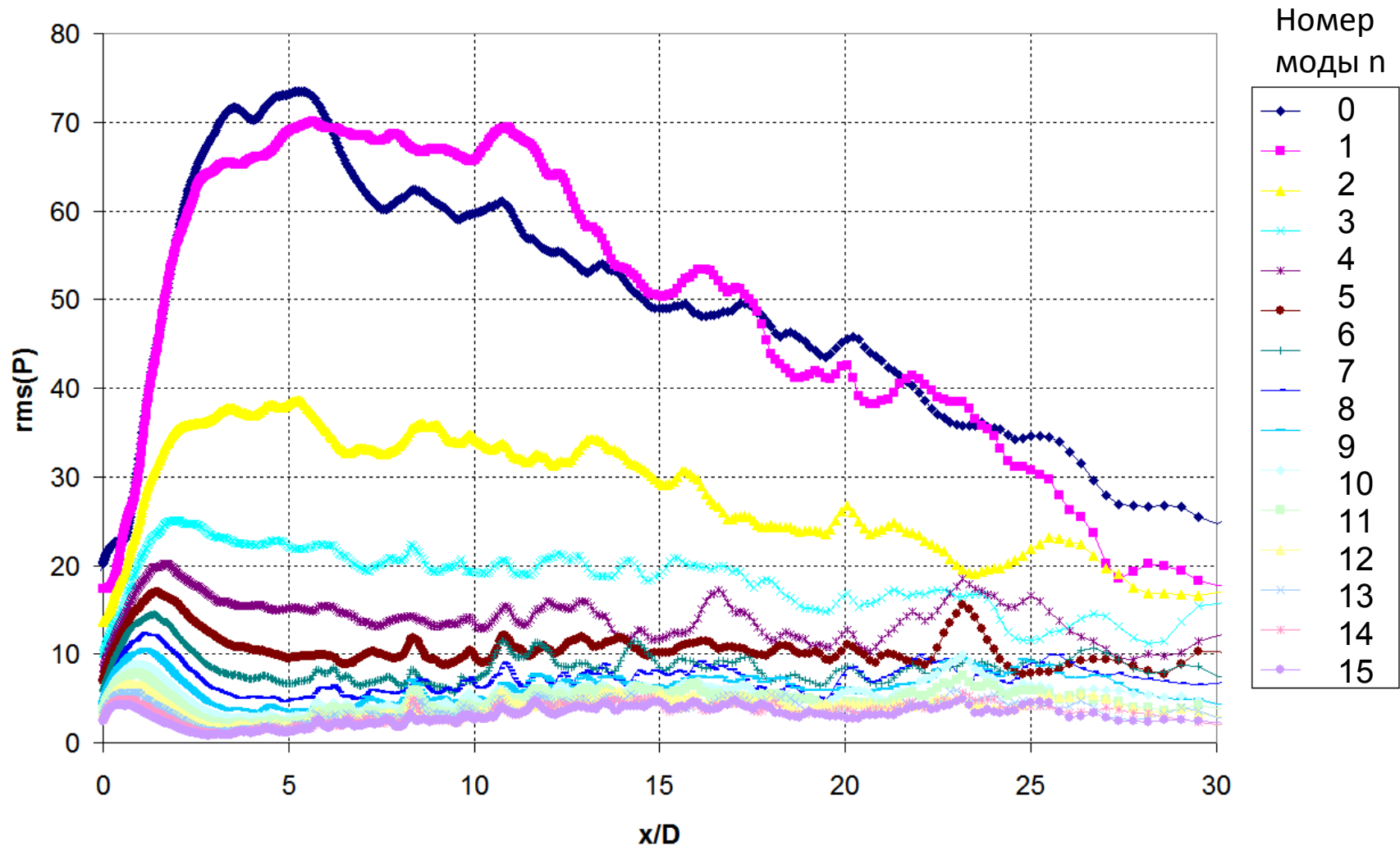
1. Cylindrical lip-line surface
2. Control FWH surfaces in the jet near field



Pressure pulsations in the near field

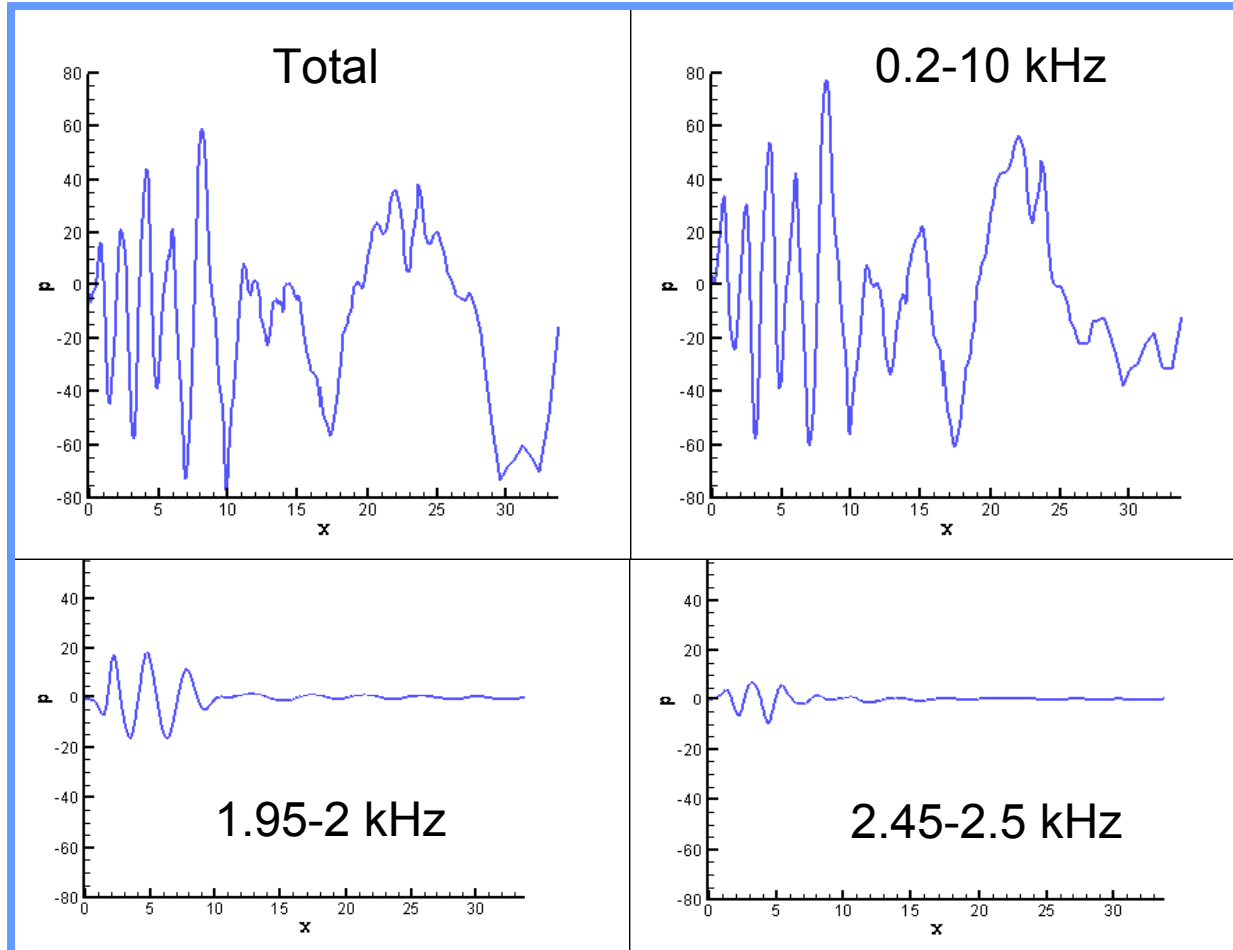


Modal content of pressure pulsations



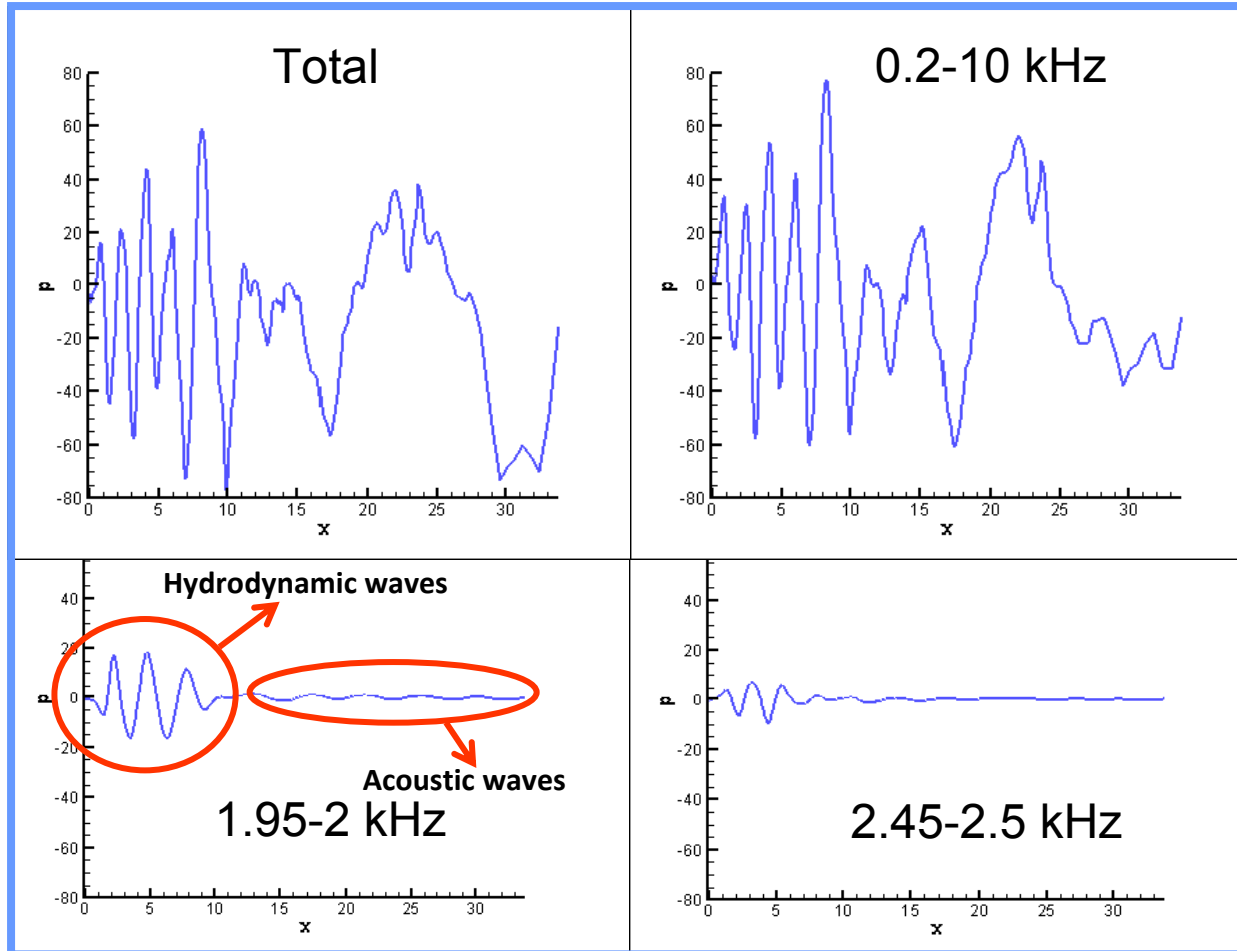
Spatio-temporal evolution of pressure pulsations, $n=0$

FWH W1, filtering in frequency bands



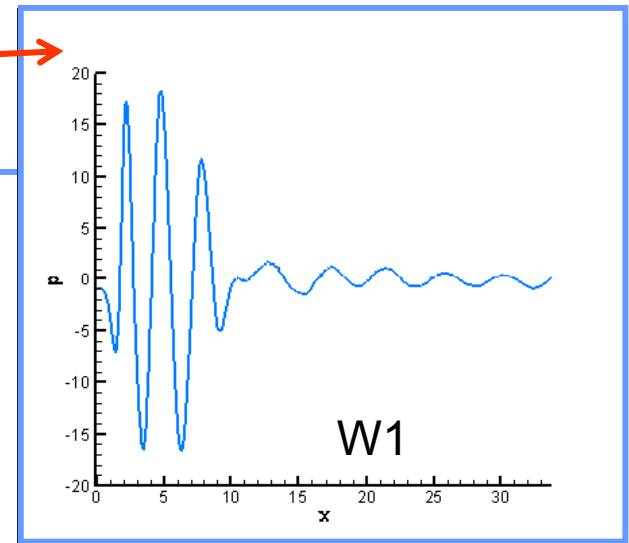
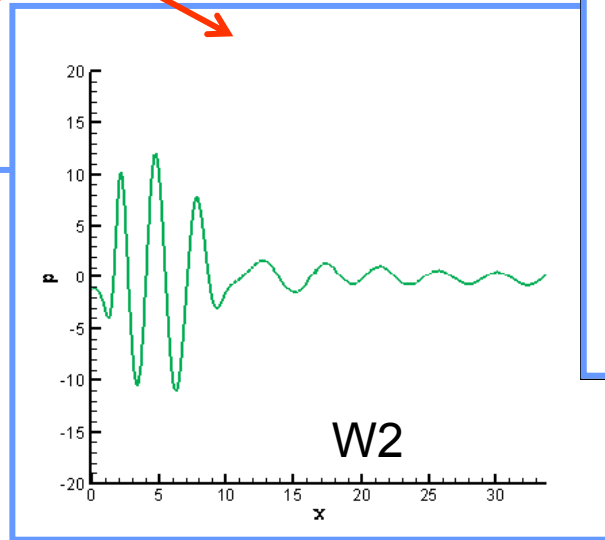
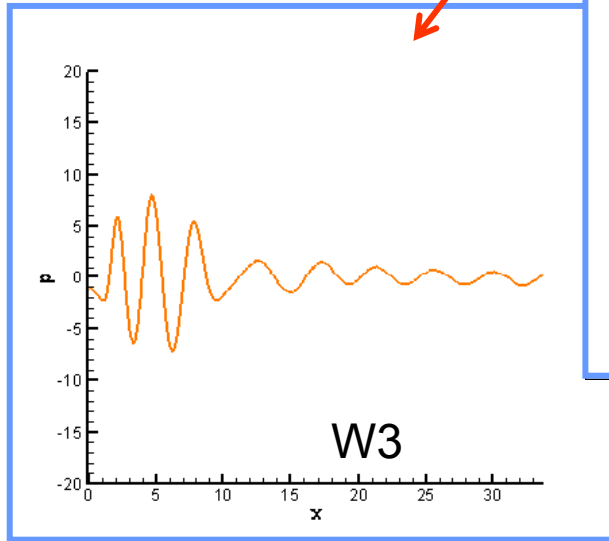
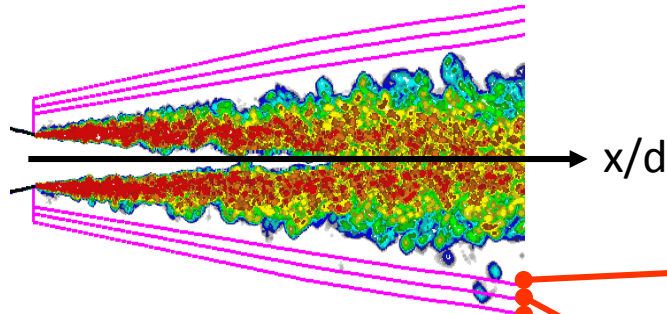
Spatio-temporal evolution of pressure pulsations, $n=0$

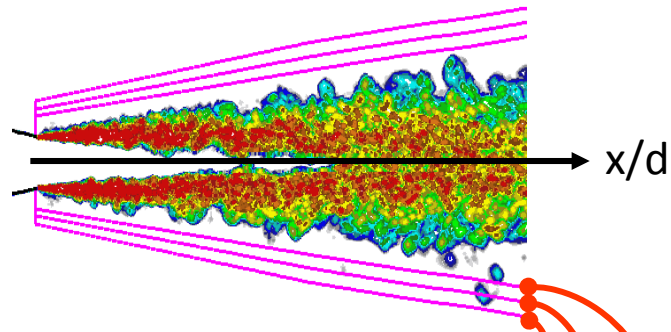
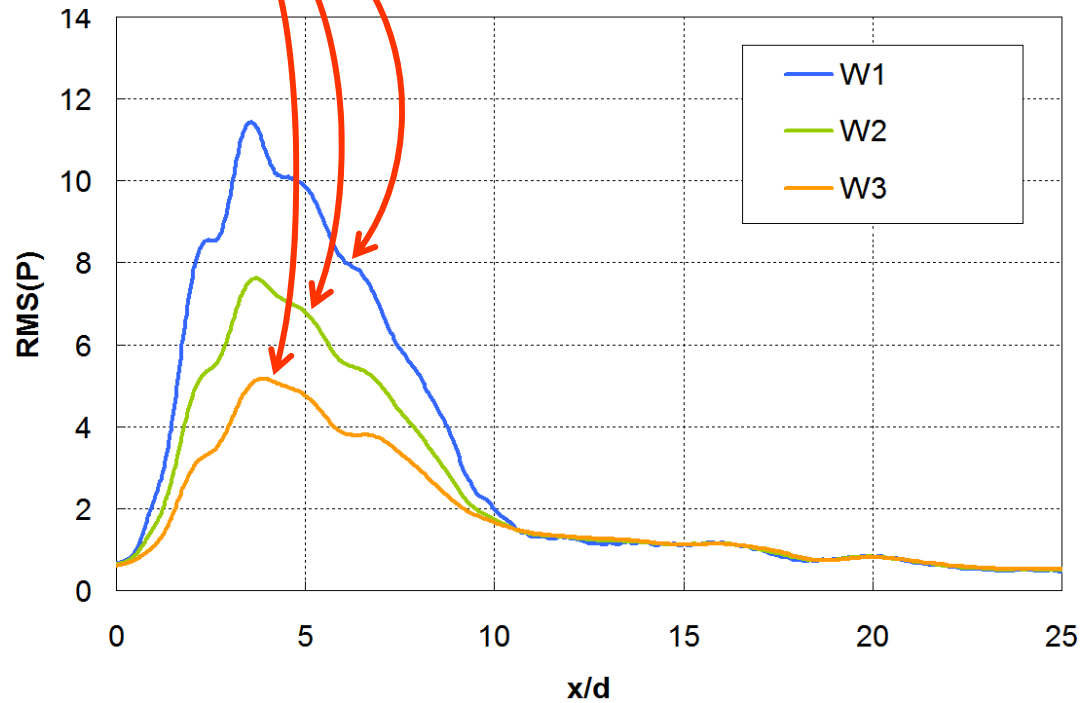
FWH W1, filtering in frequency bands



Spatio-temporal evolution of pressure pulsations, $n=0$

Frequency band $f=1.95-2$ kHz

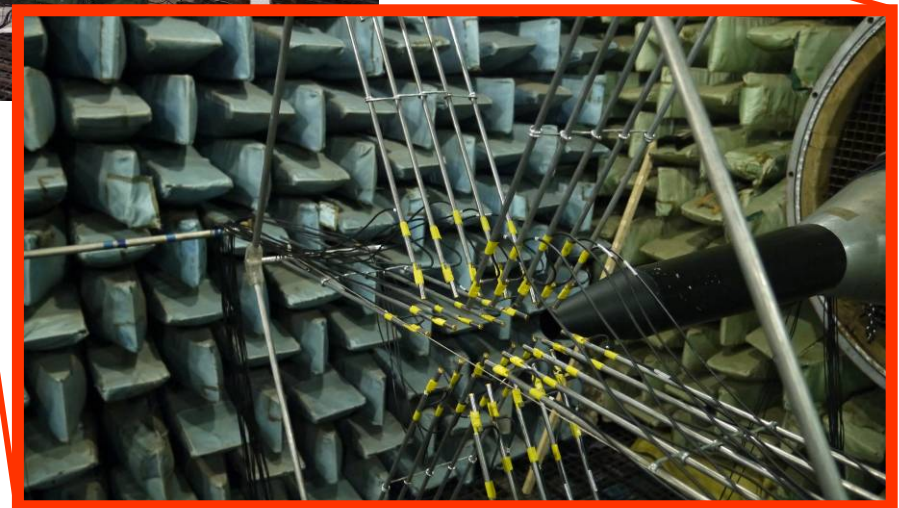
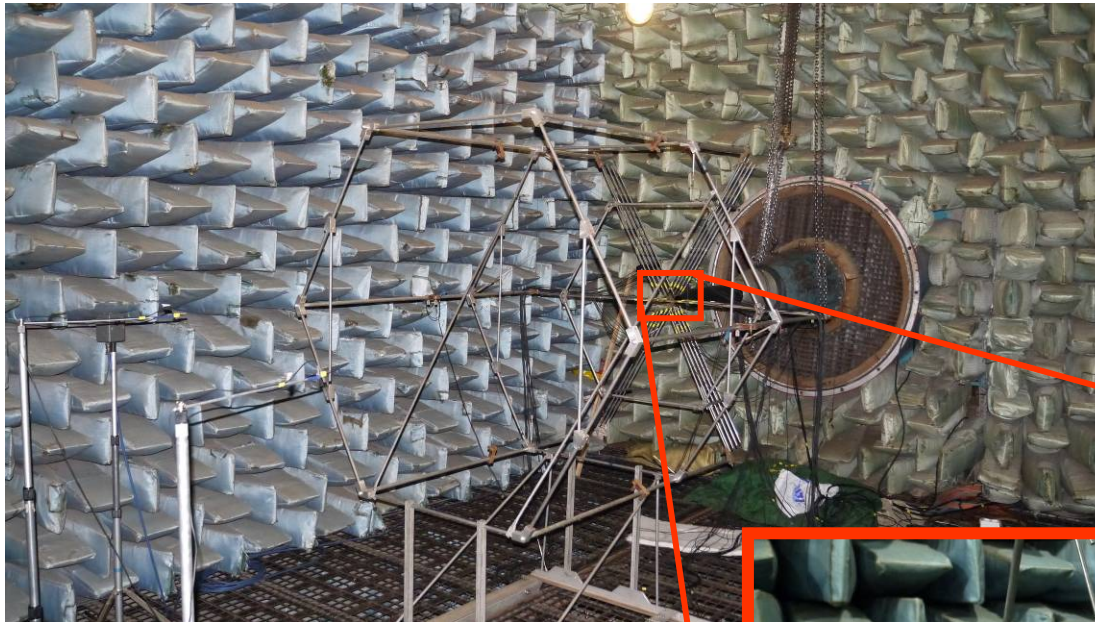


Spatio-temporal evolution of pressure pulsations, $n=0$ Frequency band $f=1.95-2$ kHz

Outline

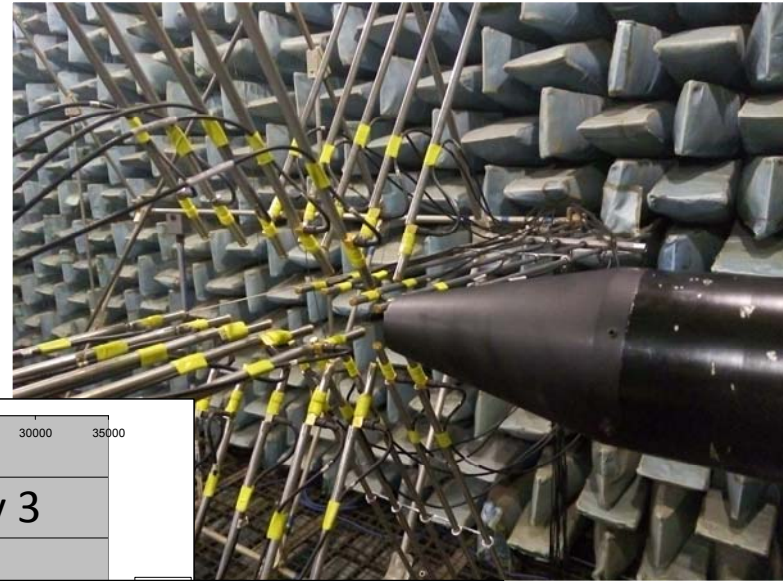
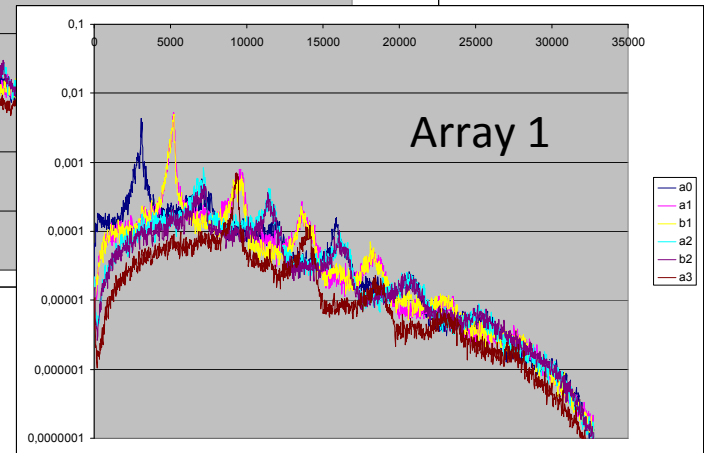
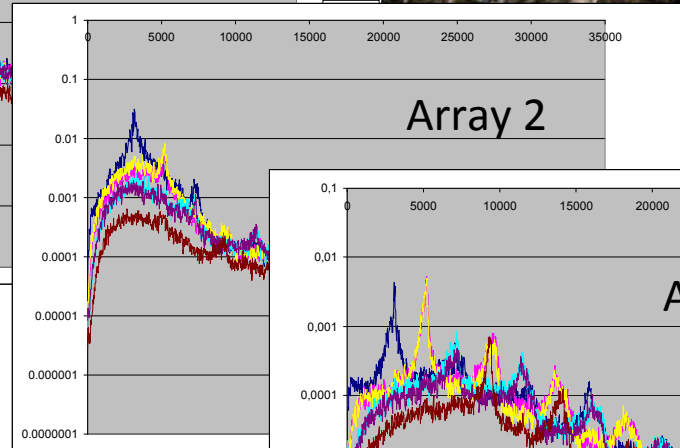
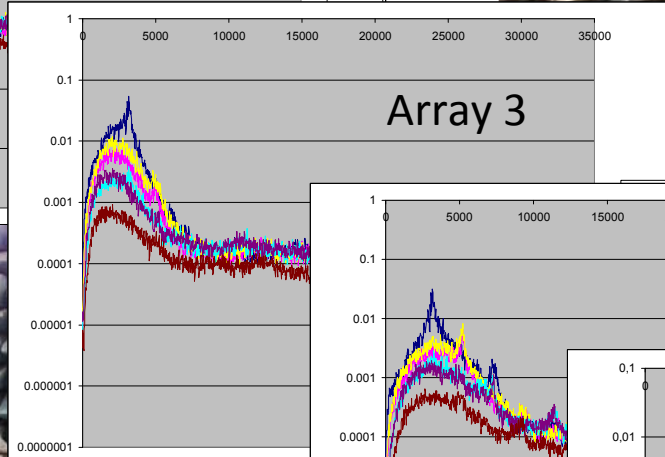
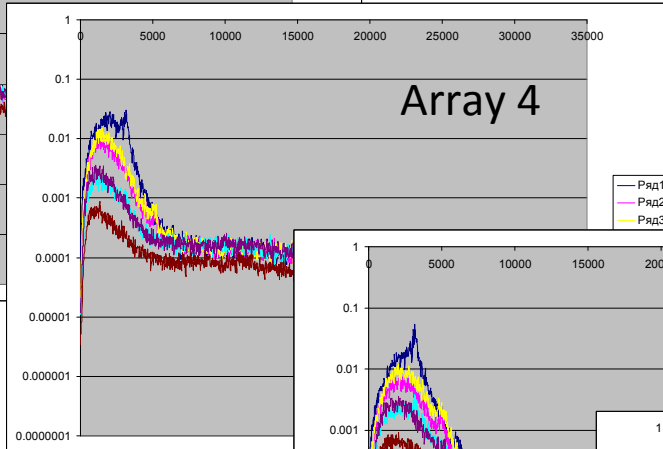
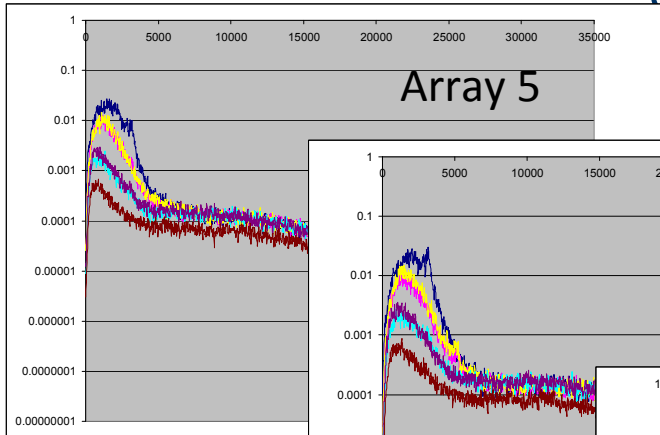
- Introduction
- Artificial instability waves (AIW) , AIW control strategy
- NIW control idea, Overview of LES-results,
- Data analysis in the jet shear layer
- Data analysis in the jet near field
- **Experimental data**
- NIW Control strategy
- Conclusion

Near-field multi-microphone array

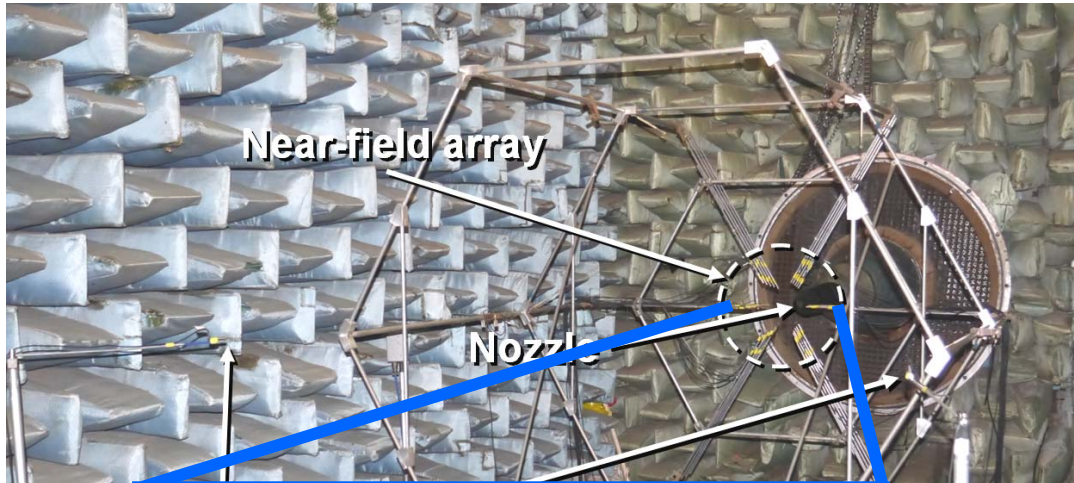


Spectra of modes

M=0.9



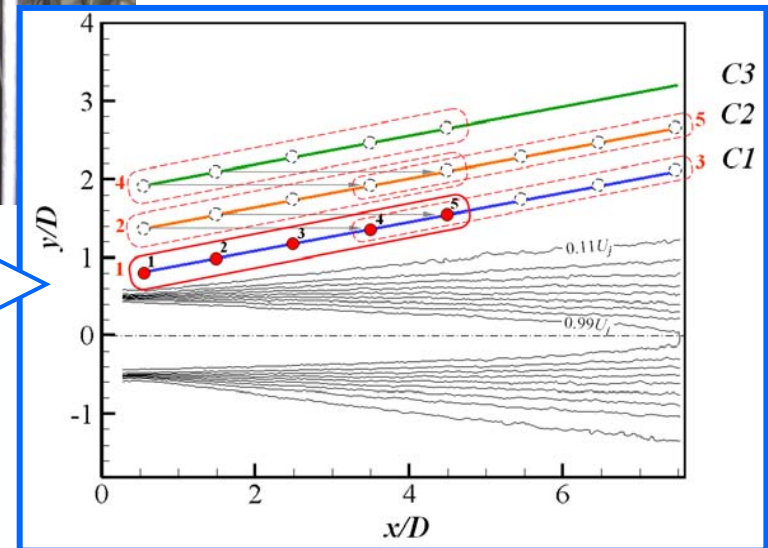
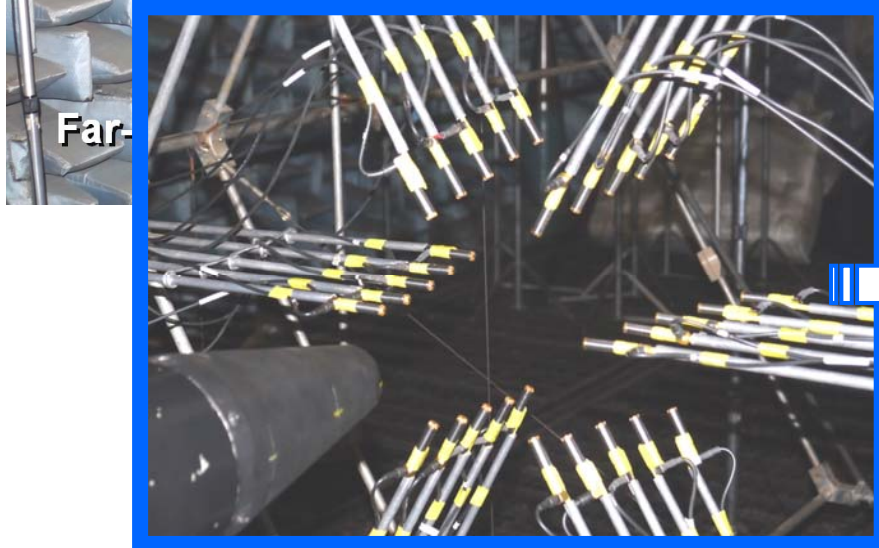
Near-field experiments



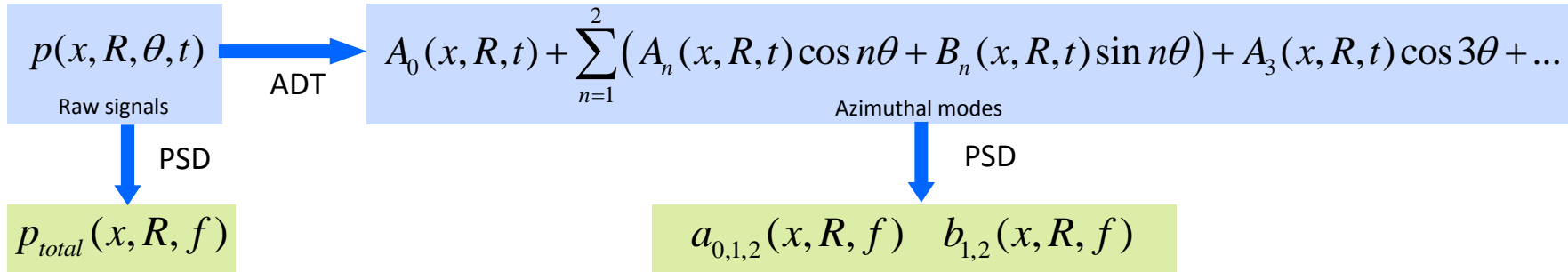
Round profiled nozzle $D=40$ mm
 Jet Mach numbers:
 $M_j=0.4, 0.53, 0.6, 0.74, 0.82, 0.9$

30 microphones:

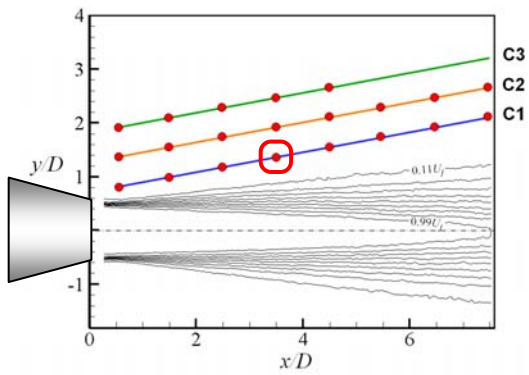
- 3 conical surfaces (C1, C2, C3)
- 5 array positions
- $x/D=0.5, 1.5, \dots, 7.5$



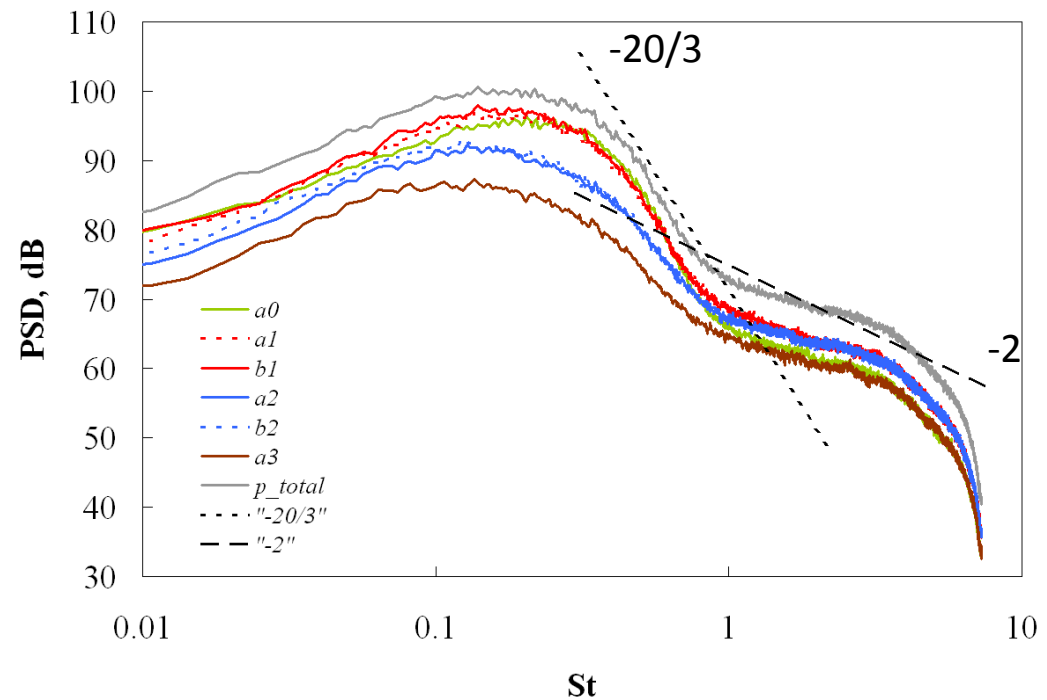
Near-field experiments



Typical near-field spectra of the total signal and its azimuthal modes. $M_j = 0.53$

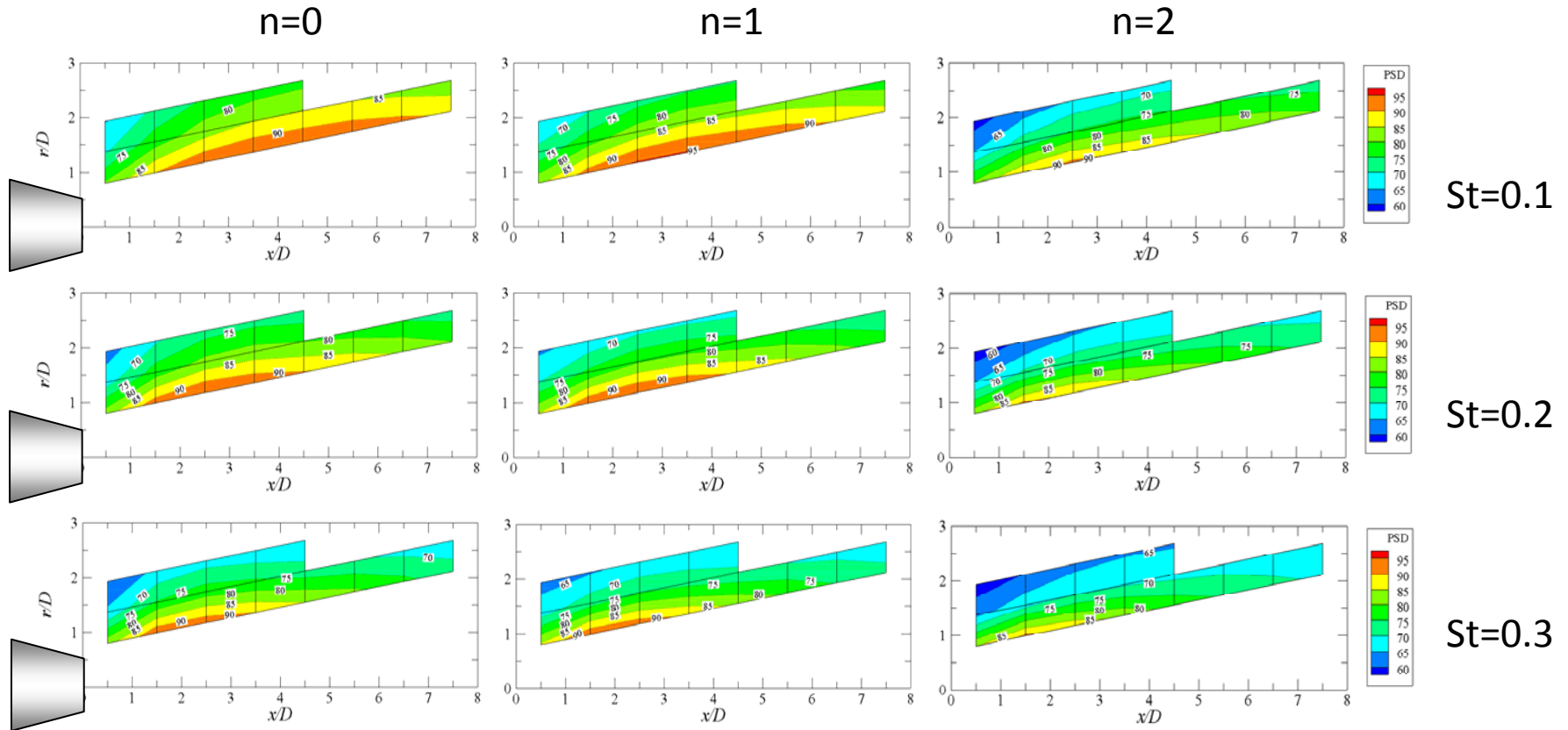


Arndt et al. 1997



Near-field experiments

Azimuthal modes $M_j=0.53$

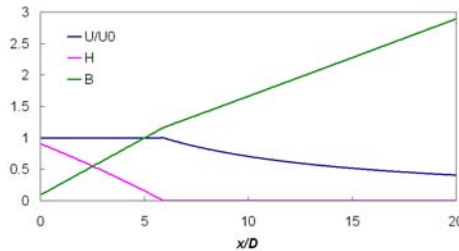


Near-field experiments

Azimuthal modes $M_j=0.53$

$n=0$

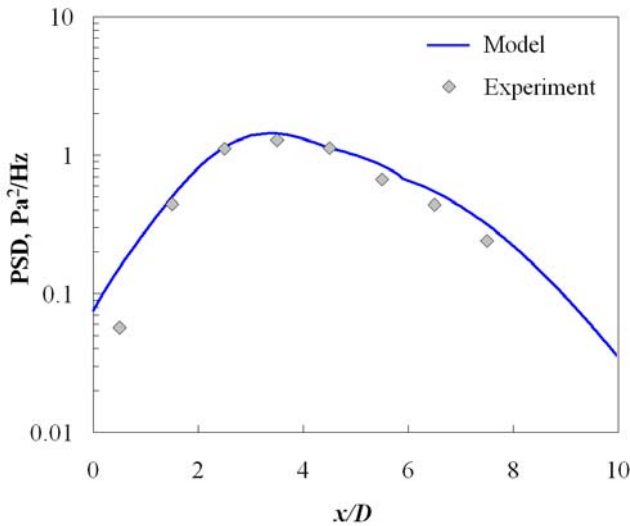
Linear stability analysis - generalized Tam's theory (AIAA 2006-2595)



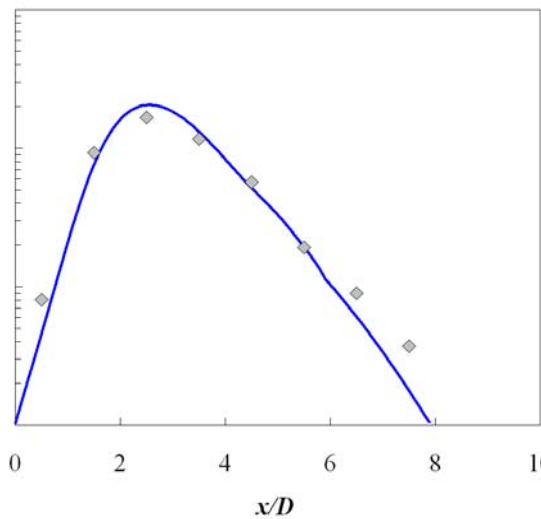
$$p \sim A(0) \sqrt{\frac{I_1(0)}{I_1(s)}} \cdot \exp\left(-\int_0^s \frac{I_0}{I_1} ds\right) \cdot \exp(-i \int \alpha ds)$$

$$p = \int_{-\infty}^{\infty} g(\eta) H_n^{(1)}(i \lambda r) \exp i\left(\eta z + \frac{\pi}{2}\right) dz$$

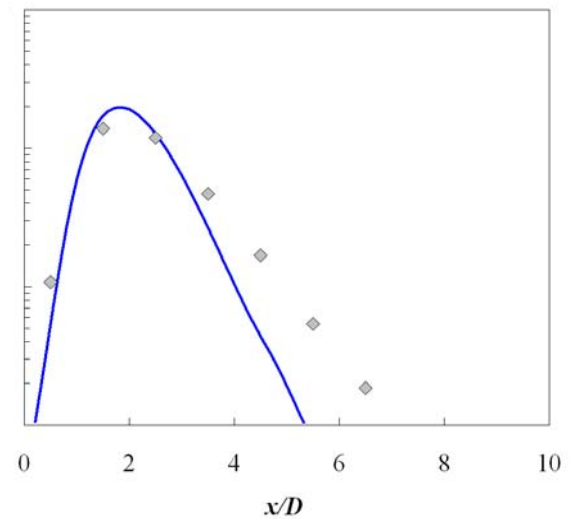
St=0.2



St=0.3



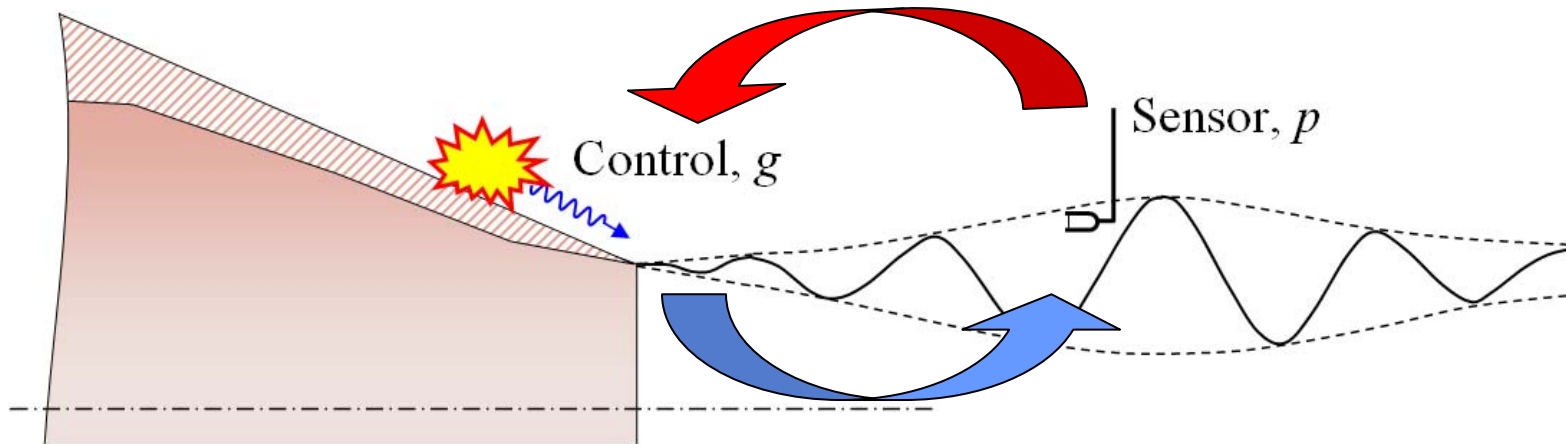
St=0.4



Outline

- Introduction
- Artificial instability waves (AIW) , AIW control strategy
- NIW control idea, Overview of LES-results,
- Data analysis in the jet shear layer
- Data analysis in the jet near field
- Experimental data
- **NIW Control strategy**
- Conclusion

Control strategy for NIW



Actuator – near the nozzle edge

Sensor – downstream from the nozzle exit

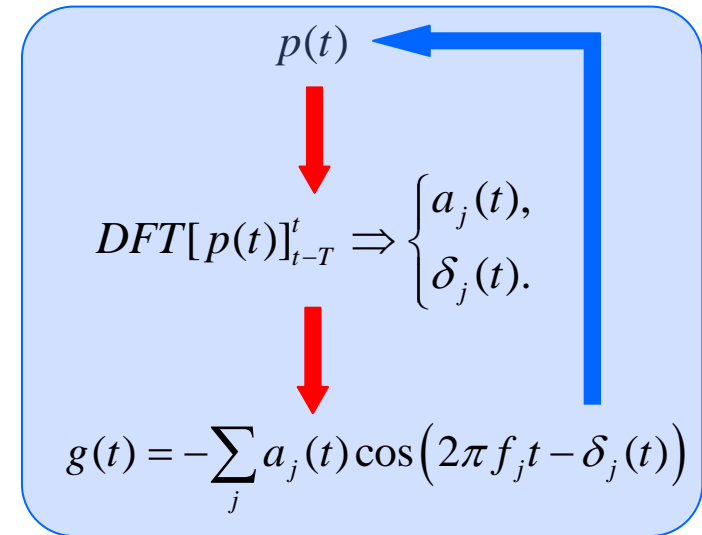
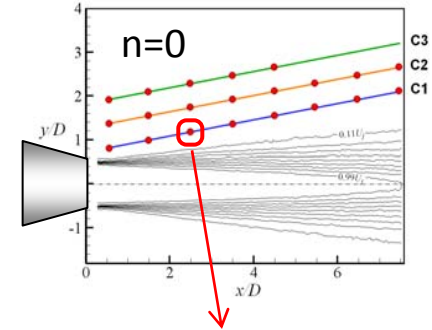
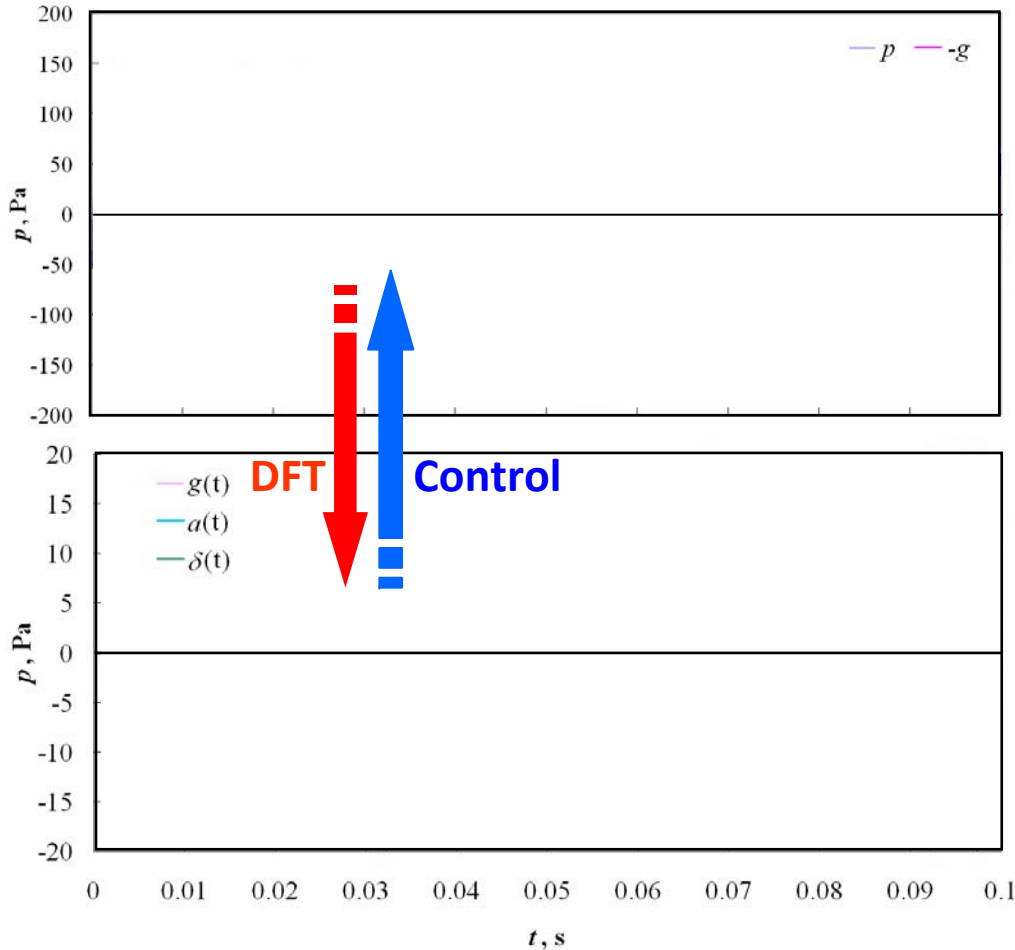
- + • Effective control action – high receptivity of the shear layer
- • Inevitable time delay $\tau \sim D/V_c$, ($\tau \sim 0.3$ ms for $M_j = 0.53$)

Control of model signal in a narrow frequency band

$f_c = 65.536 \text{ kHz}$ – sampling rate

$N_{\text{DFT}} = 2048$ points – $\Delta f = 32 \text{ Hz}$

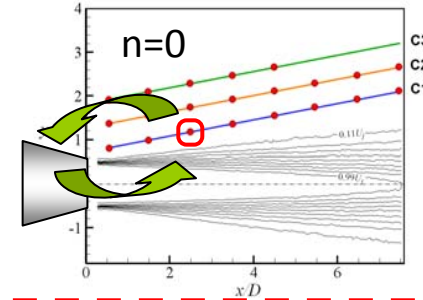
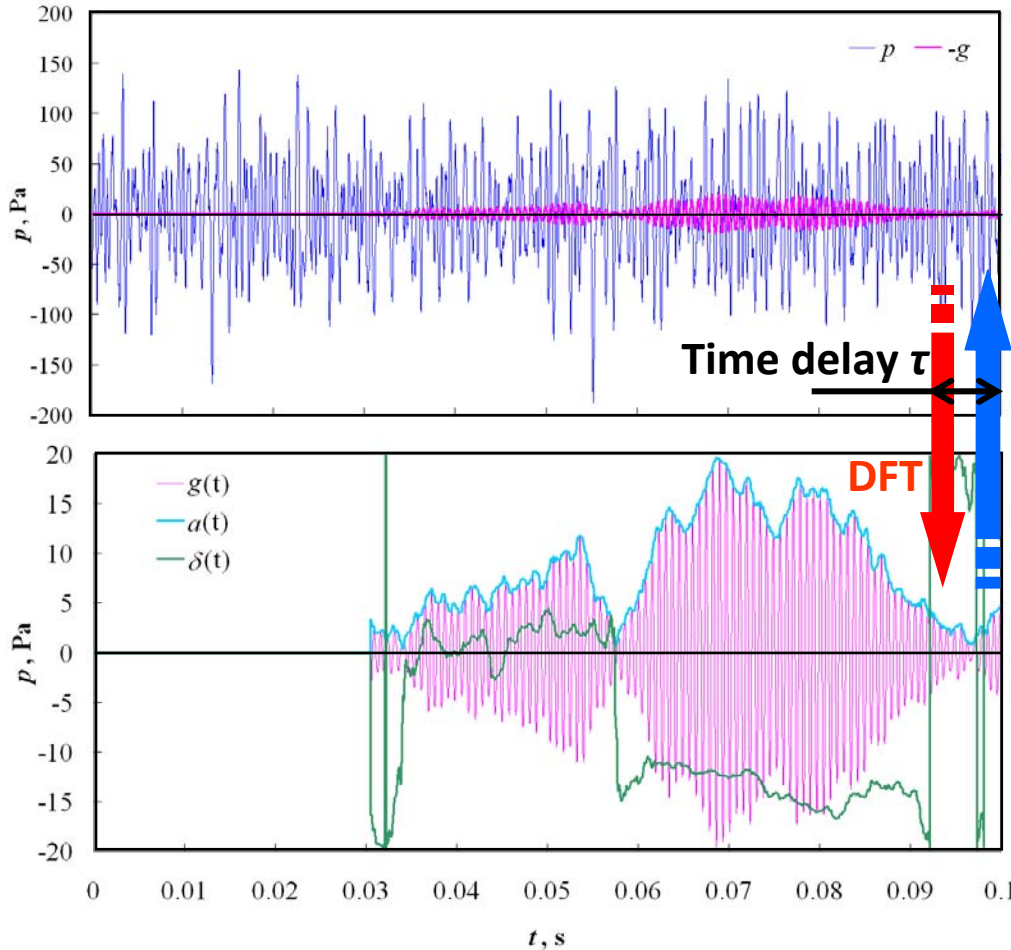
Control at $St = 0.3$



Control of model signal in a narrow frequency band

$f_c = 65.536 \text{ kHz}$ – sampling rate
 $N_{\text{DFT}} = 2048$ points – $\Delta f = 32 \text{ Hz}$

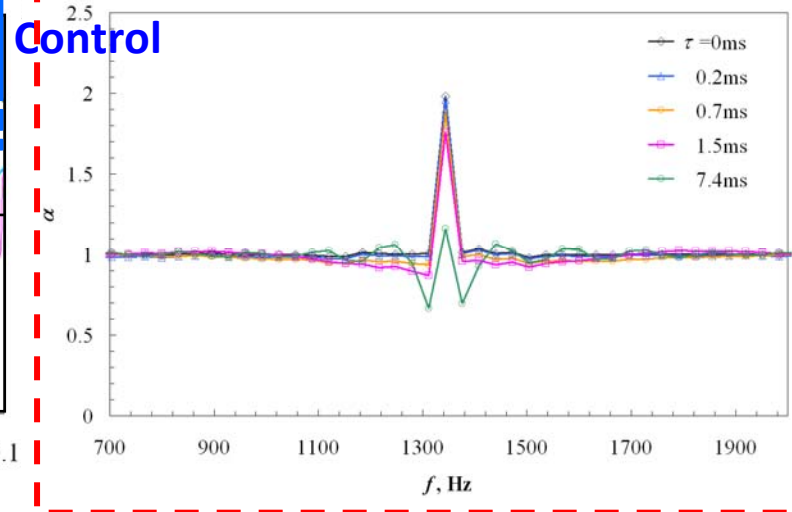
Control at $St = 0.3$



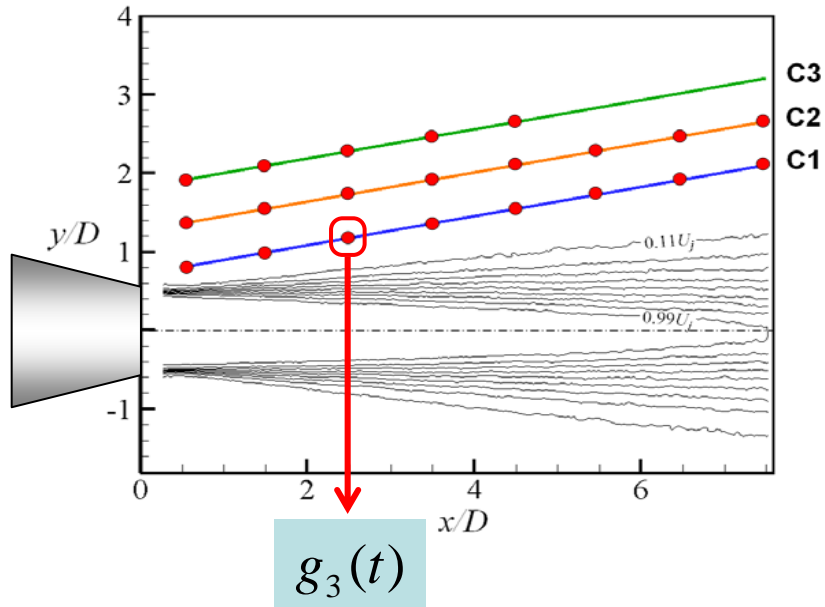
Time delay
 $\tau \sim D/V_c$

Suppression ratio for different time delays τ

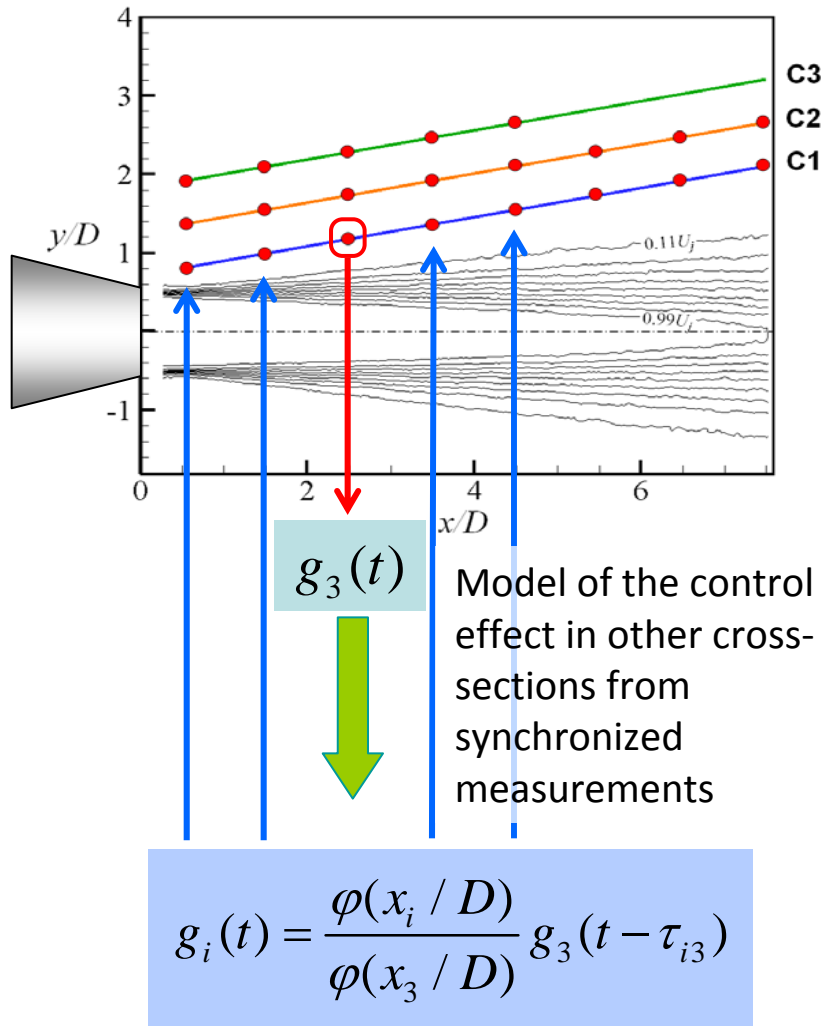
$$\alpha(f) = \frac{P_{\text{control-OFF}}(f)}{P_{\text{control-ON}}(f)}$$



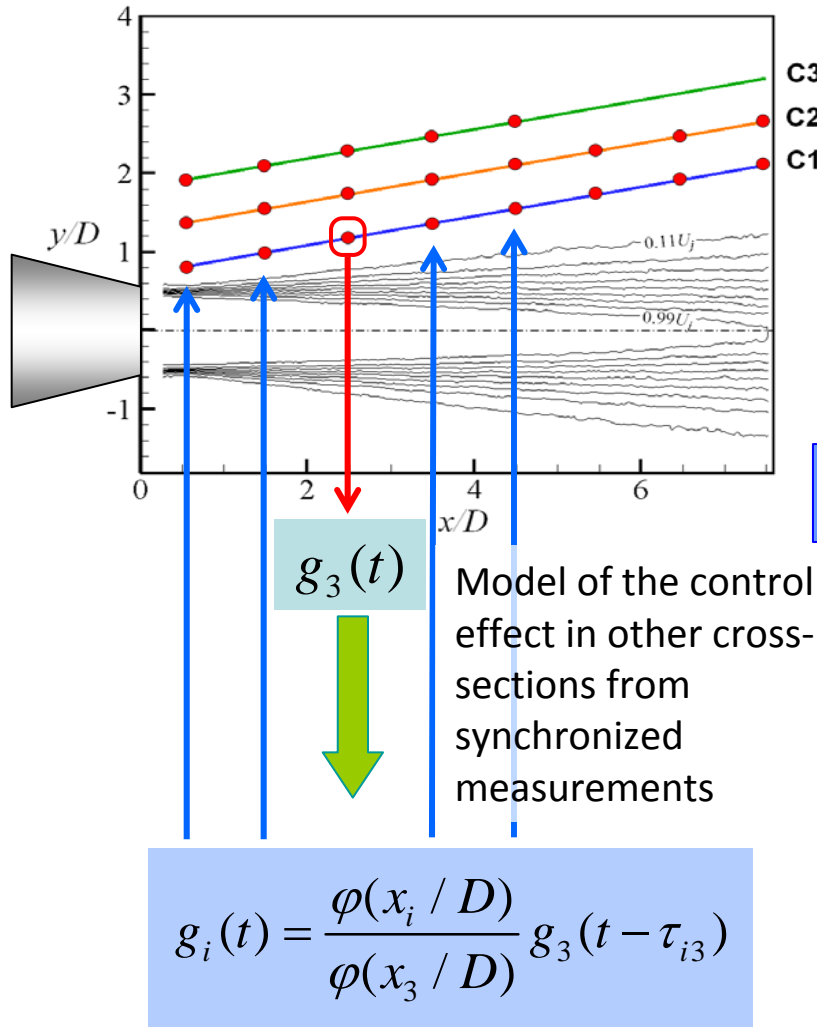
Imitation of wavepacket control in a narrow frequency band



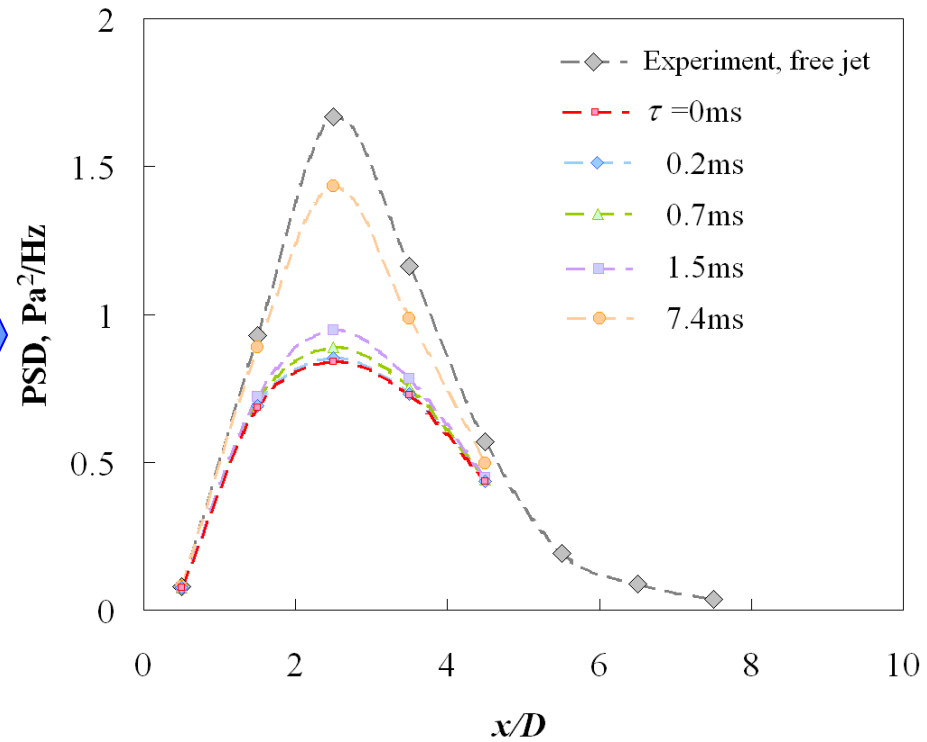
Imitation of wavepacket control in a narrow frequency band



Imitation of wavepacket control in a narrow frequency band



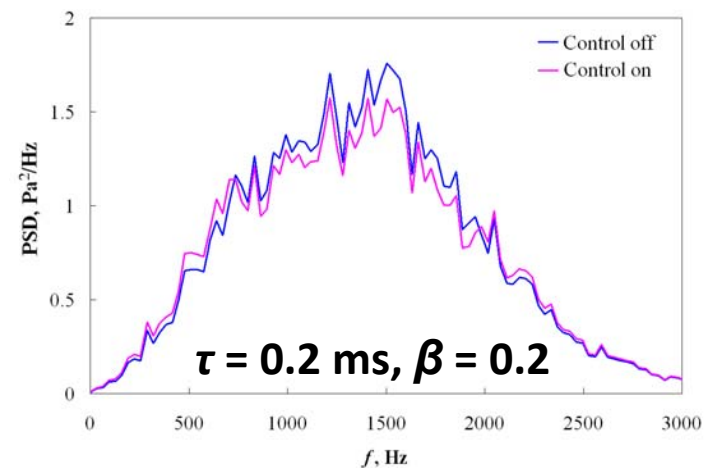
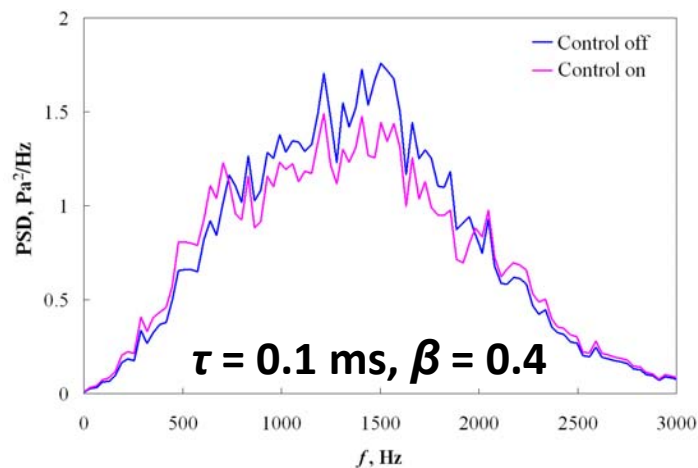
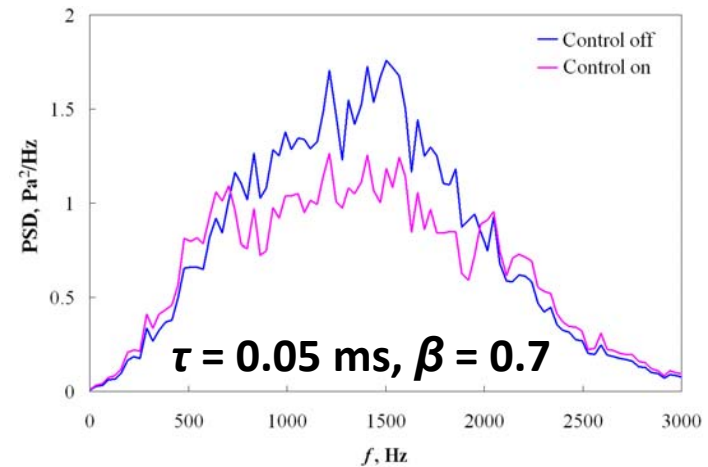
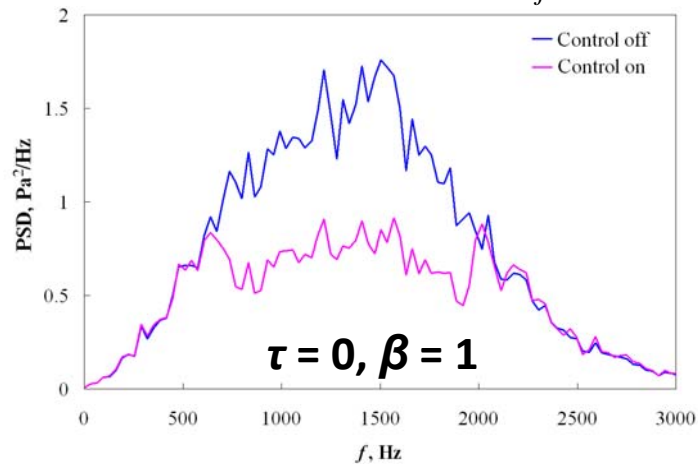
Effect of control on the wavepacket



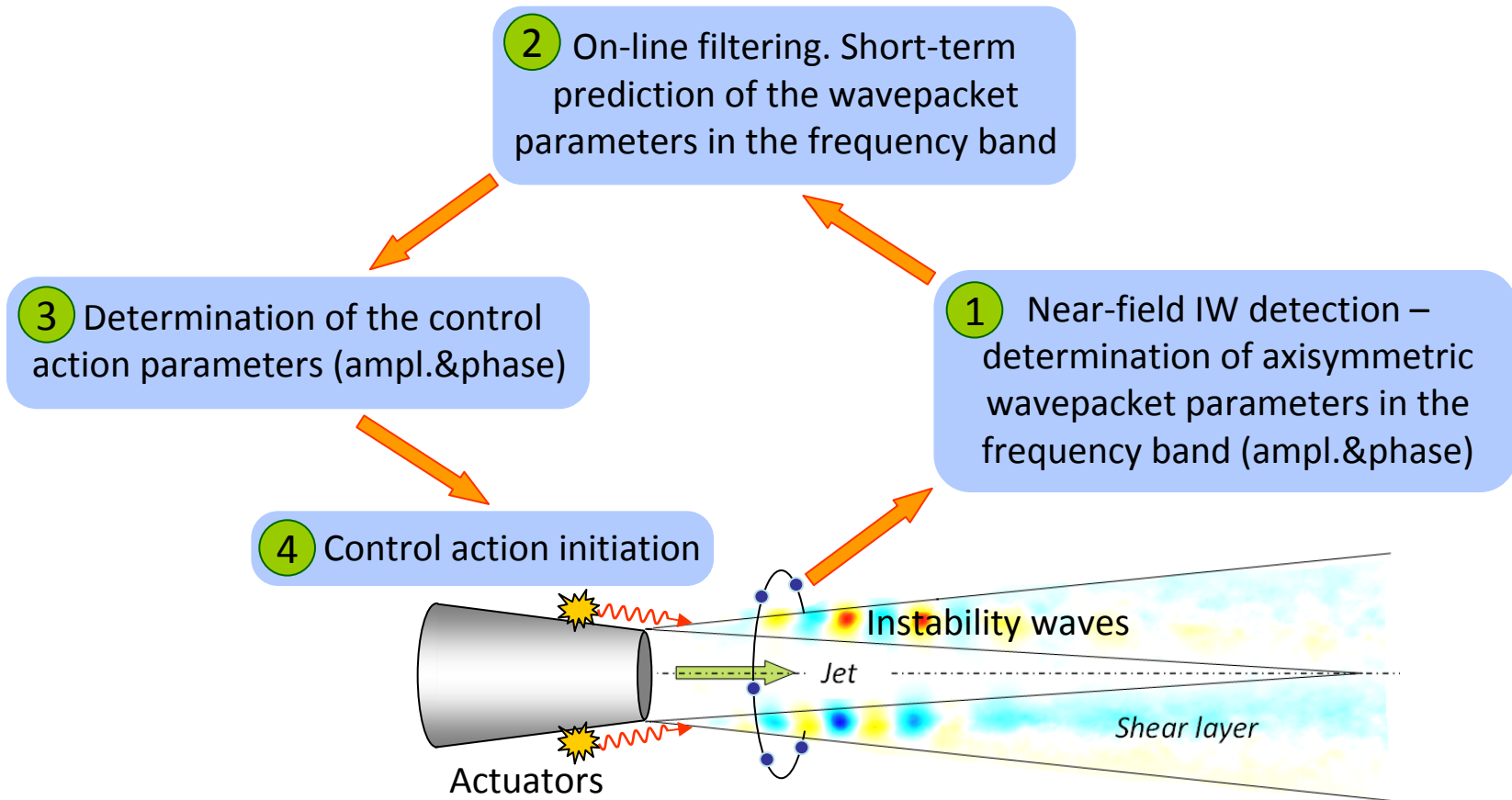
Effect of the delay at broadband control

Spectra of the controlled and uncontrolled signals (0.7-2.0kHz)

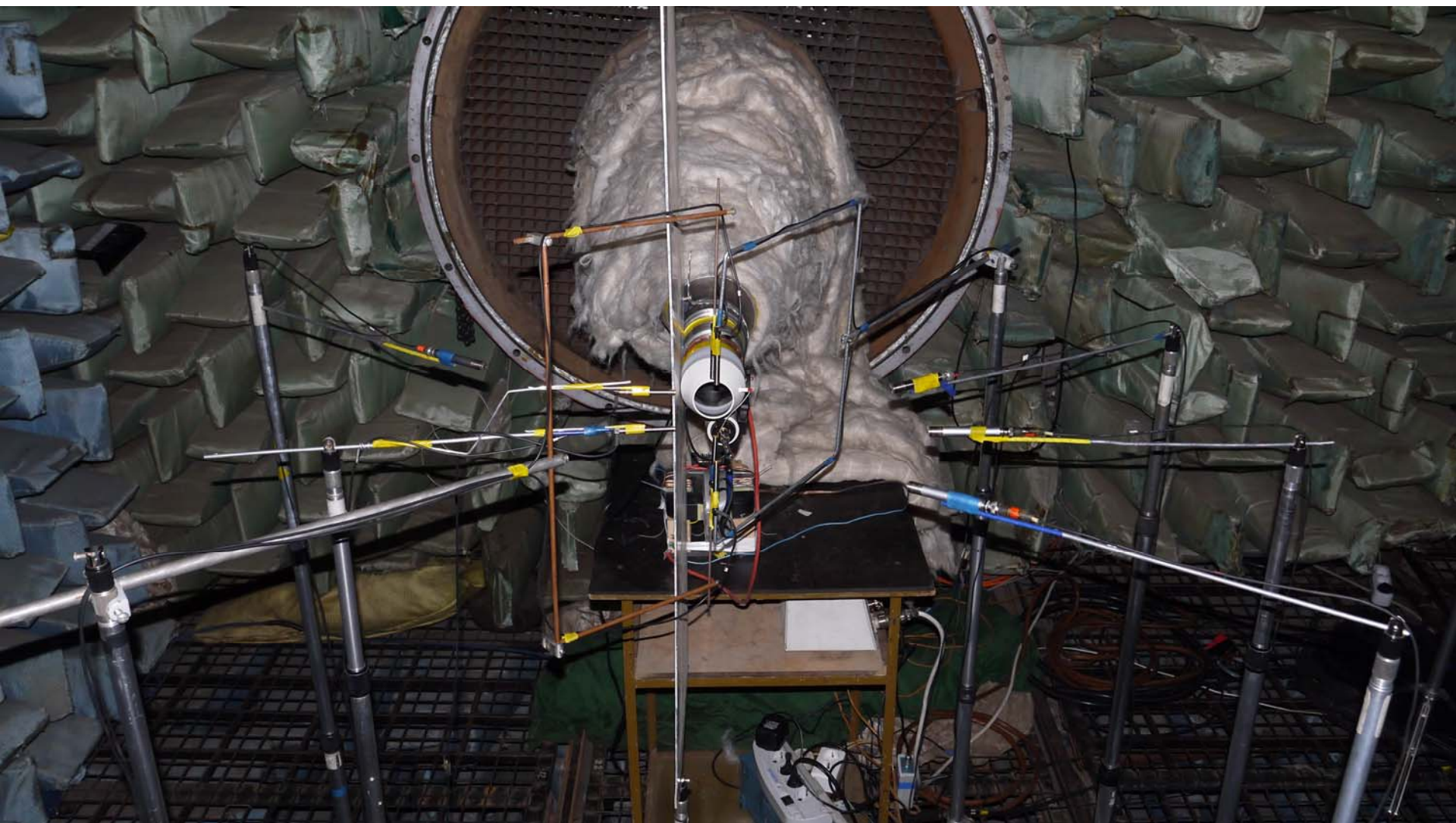
$$g(t) = -\beta \sum_j a_j(t) \cos(2\pi f_j(t + \tau) - \delta_j(t))$$



Control strategy



Control of real signal in a narrow frequency band, experimental setup TsAGI and JIHT RAS



Conclusion

- The possibility of closed-loop control of artificially excited instability waves (AIW) by linear adjustment of the excitation and the control action is demonstrated.
- Analysis of the LES data was used to design microphone array for experimental detection of natural instability waves (NIW).
- It is shown that outside the shear layer, in the jet near field, there is a region containing footprints of large-scale structures related to the Kelvin-Helmholtz instability waves in the form of wave packets of 0, 1 and 2 azimuthal modes.
- It is shown on the model signal (axisymmetric mode) taken from the near-field measurements that such approach can lead to about twofold signal reduction ($\sim 3\text{dB}$) in the given frequency band even for nonzero delay.
- It is shown that the integral effect of the control on the signal spectrum becomes negative despite the reduction in the given frequency band. This effect is related to the amplitude and phase errors introduced by the control. Reduction of the control amplitude and broadband action in the region of spectral maximum were proposed for mitigation of this time delay effect.
- It is demonstrated that the control signal defined by the measurements at one cross-section is able to suppress signals at different positions along the jet axis for moderate time delays, i.e. the control allows approximately twofold reduction of the wavepacket amplitude.